
DETECTING HIDDEN CONFOUNDING IN OBSERVATIONAL DATA USING MULTIPLE ENVIRONMENTS

Rickard K.A. Karlsson
Delft University of Technology
The Netherlands
r.k.a.karlsson@tudelft.nl

Jesse H. Krijthe
Delft University of Technology
The Netherlands
j.h.krijthe@tudelft.nl

May 30, 2023

ABSTRACT

A common assumption in causal inference from observational data is that there is no hidden confounding. Yet it is, in general, impossible to verify this assumption from a single dataset. Under the assumption of independent causal mechanisms underlying the data-generating process, we demonstrate a way to detect unobserved confounders when having multiple observational datasets coming from different environments. We present a theory for testable conditional independencies that are only absent when there is hidden confounding and examine cases where we violate its assumptions: degenerate & dependent mechanisms, and faithfulness violations. Additionally, we propose a procedure to test these independencies and study its empirical finite-sample behavior using simulation studies and semi-synthetic data based on a real-world dataset. In most cases, the proposed procedure correctly predicts the presence of hidden confounding, particularly when the confounding bias is large.

1 Introduction

Estimating the causal effect of a treatment on an outcome is a fundamental challenge in many areas of science and society. While this is straightforwardly done using data from randomized studies, using observational data for this task is appealing since they are often more feasible to collect while also being more representative of the population of interest (Pearl, 2009). To identify causal effects using such data it is often assumed there is no hidden confounding. When this *untestable* assumption is violated we run the risk of confusing causal relationships with spurious correlations. This can have serious consequences such as unknowingly suggesting a non-effective or, even worse, potentially harmful treatment. Therefore, detecting the presence of hidden confounding is an important problem.

Data collected from different sources often tend to be heterogeneous due to e.g. changing circumstances or time shifts. In this work, we show how such heterogeneity can be exploited to make hidden confounding testable *solely* from observational data. We consider a setting where observational data has been collected from different environments E . In each environment, we observe the same treatment T and outcome Y , as well as covariates X that are known confounders between T and Y . Further, we assume that the data is heterogeneous across these environments under the principle of *Independent Causal Mechanisms* (Peters et al., 2017; Schölkopf et al., 2021), which states that a causal system consists of autonomous modules that do not inform or influence each other. The question we ask is whether there exists further hidden confounding between T and Y after having adjusted for X . If that is the case, the causal effect of T on Y is not identifiable in general. Perhaps surprisingly, we demonstrate a way to decide if the causal effect would be identifiable by deriving testable implications for whether hidden confounding is present or not. We achieve this by exploiting the hierarchical structure of the problem, shown in Figure 1.

As an illustration of a setting where this might be applied, imagine a situation where we have collected observational data for a specific treatment and outcome from multiple hospitals that care for patients in different demographics. As a consequence, we might suspect the existence of potential confounders such as income status or health-seeking

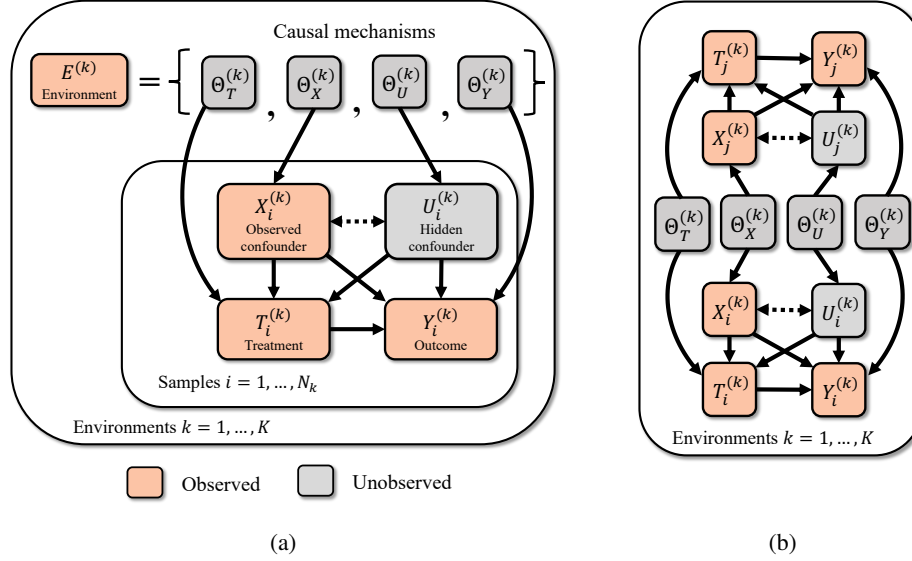


Figure 1: We have multiple observations $i = 1, \dots, N_k$ of treatment $T_i^{(k)}$, outcome $Y_i^{(k)}$ and confounder $X_i^{(k)}$ in different environments $E^{(k)}$. The dashed bi-directed edge between $X_i^{(k)}$ and $U_i^{(k)}$ allows for any causal relationship, or lack thereof, between the observed and hidden confounder. (a): The hierarchical structure of the multi-environment data; the causal mechanisms are unobserved but we know the indicator $E^{(k)}$ for what environment observations belong to. (b): By unrolling the graph in (a) we see that dependencies exist between any pairs of observations (i, j) from the same environment (when not conditioning on the mechanisms). This can be exploited to detect the presence of the hidden confounder.

behavior. This scenario can come up in meta-analyses with multiple observational studies where no randomized control trials are available, a problem area where systematic procedures are still lacking (Mueller et al., 2018). Now, if these potential confounding factors have different distributions at each hospital, our work proposes a way to statistically test the presence of confounding – even when we do not observe the confounding factors directly.

Contributions We prove that there exists, under the principle of independent causal mechanisms, testable independencies that are only violated in the presence of unobserved confounding between treatment and outcome (Sec. 4, Theorem 1). Further, we explore the effect of changes and violations of our assumptions – while most assumptions are necessary, we find that some can be relaxed (Sec. 4.1). We then introduce a statistical testing procedure that uses any suitable conditional independence test to detect the presence of hidden confounding in observational datasets from multiple environments (Sec. 4.2). Lastly, we perform an empirical finite-sample analysis of it using both synthetic and semi-synthetic data generated with real-world covariates from the Twins dataset (Almond et al., 2005; Louizos et al., 2017). We observe that our proposed procedure correctly predicts the presence of hidden confounding in most cases, particularly when the confounding bias is large (Sec. 5).

2 Problem setting

We start with some preliminaries of the causal terminology used in this paper.

Definition 1 (Causal Graphical Model (CGM)). A causal graphical model $M = (\mathcal{G}, P)$ over d random variables $\mathbf{V} = (V_1, V_2, \dots, V_d)$ comprises (i) a directed acyclic graph (DAG) \mathcal{G} with vertices \mathbf{V} and edges $V_i \rightarrow V_j$ iff V_i is a direct cause of V_j , and (ii) a joint distribution P such that it has the following Markov or causal factorization over \mathcal{G} :

$$P(V_1, V_2, \dots, V_d) = \prod_{i=1}^d P(V_i \mid \text{Pa}(V_i)) \quad (1)$$

where $\text{Pa}(V_i)$ denotes the parents (direct causes) of V_i in \mathcal{G} and $P(V_i \mid \text{Pa}(V_i))$ is the causal mechanism of V_i .

The DAG \mathcal{G} encodes various conditional independencies between the variables – also known as d-separations in the DAG, see Pearl (1988, Chapter 3.3) – which we write as $\mathbf{A} \perp\!\!\!\perp_d \mathbf{B} \mid \mathbf{C}$ over some disjoint sets of variables \mathbf{A} , \mathbf{B} and \mathbf{C} . We shall assume that conditional independencies in \mathcal{G} imply the same conditional independencies in P , and vice versa:

Assumption 1 (Faithfulness & Causal Markov Property). *For P and \mathcal{G} we have (i) the faithfulness property that $\mathbf{A} \perp\!\!\!\perp_P \mathbf{B} \mid \mathbf{C} \Rightarrow \mathbf{A} \perp\!\!\!\perp_d \mathbf{B} \mid \mathbf{C}$, and (ii) the causal Markov property that $\mathbf{A} \perp\!\!\!\perp_P \mathbf{B} \mid \mathbf{C} \Leftarrow \mathbf{A} \perp\!\!\!\perp_d \mathbf{B} \mid \mathbf{C}$.*

We consider a setting with the following variables in our causal graphical model: a one-dimensional treatment $T \in \mathcal{T}$ and outcome $Y \in \mathcal{Y}$, in addition to some observed covariates $X \in \mathcal{X}$ and unobserved covariates $U \in \mathcal{U}$. We do not restrict the dimensionality of X and U . Additionally, in this setting, the environment E has a direct effect on all other variables, making it a root node in \mathcal{G} . We say that a variable is a confounder between T and Y if it is a cause of both T and Y in \mathcal{G} . We assume that X is a known confounder between T and Y , while the relationship between U and the other variables is unknown. Hence, U could be an unobserved hidden confounder (as illustrated in Figure 2) or, for instance, completely unrelated to the other variables.

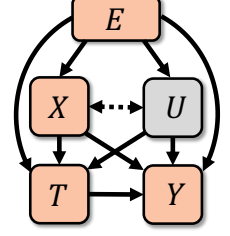


Figure 2: The setting where we want to detect the presence of a hidden confounder U in \mathcal{G} .

Expressed in the framework of Pearl (2009), the goal of causal inference is to estimate the probability $P(Y \mid do(T = t))$ where $do(T = t)$ represents an intervention on the treatment. Without any further assumptions, $P(Y \mid do(T = t))$ is not identifiable from an observational dataset; that is data where we have observed the choice of treatment without influencing it (Pearl, 2009). In particular, in the setting we consider here, the interventional effect remains unidentifiable if the unobserved U is a confounder between T and Y .¹ Unfortunately, there is no way to check whether such unobserved confounders are present in a single dataset. We will show, however, that things are different when we have access to observational datasets from multiple environments. In this setting, we present a way to detect confounding even if it is not observed, hence demonstrating a novel and valuable approach for verifying an essential prerequisite for causal inference from observational data. In the rest of this section, we present the main assumptions that enable us to do this.

First, we have data from multiple environments $E \in \mathcal{E}$ with different joint distributions $P(T, Y, X, U \mid E)$. We shall use $P_E(\cdot)$ to denote $P(\cdot \mid E)$, and use small letters for the random variables whenever they take particular values. In our setting, we have datasets $D_k = \{t_i^{(k)}, y_i^{(k)}, x_i^{(k)}\}_{i=1}^{N_k}$ from multiple environments $e^{(1)}, e^{(2)}, \dots, e^{(K)}$; each has N_k observations which are assumed to be i.i.d. within the environment. N_k is fixed but can be different for each environment. The environments are related to each other through the following assumption.

Assumption 2 (Shared Causal Graph). *All environments share the same underlying causal DAG \mathcal{G} .*

Next, we specify how changes in $P_E(T, Y, X, U)$ arise between the different environments. We shall assume that the conditional probabilities in (1) – which we refer to as causal mechanisms – vary independently per environment. This is known as the independent causal mechanism principle.

Assumption 3 (Independent Causal Mechanism (ICM) Principle (Peters et al., 2017)). *The causal generative process of a system’s variables is composed of autonomous modules that do not inform or influence each other. In the probabilistic case, this means that the conditional distribution of each variable given its causes (i.e., its parents in the causal graph) does not inform or influence the other mechanisms.*

The above assumption covers two aspects: one concerning *informing* and the other about *influencing*. That the mechanisms do not *inform* each other can be interpreted as that knowing the conditional probability of one variable does not tell us anything about the conditional probabilities of other variables (Janzing and Schölkopf, 2010; Guo et al., 2022). Further, we assume that changing (or performing an intervention upon) one mechanism has no *influence* on other mechanisms (Schölkopf et al., 2012). While this notion of independence between mechanisms can be described through a non-stochastic, algorithmic mutual information (Janzing and Schölkopf, 2010), we focus in this work explicitly on statistically independent mechanisms.

¹There exist other procedures that could circumvent this issue, but these alternatives seldom avoid the unconfoundedness assumption completely. As an example, instrumental variable estimation is applicable when there is unobserved confounding between T and Y , but only when the relationship between the instrumental variable and T is unconfounded (Angrist et al., 1996).

To model changes between environments with independent causal mechanisms, we parameterize each causal mechanism with $\Theta_V \in \mathcal{O}_V$ for $V \in \{T, Y, X, U\}$. Then, we define the environment variable as $E = (\Theta_T, \Theta_Y, \Theta_X, \Theta_U)$ such that

$$P_E(T, Y, X, U) = \prod_{V \in \{T, Y, X, U\}} P_{\Theta_V}(V \mid \text{Pa}(V)) . \quad (2)$$

Note that while we need to know which observations come from which environment, we do not assume to know anything about the individual parameters $(\Theta_T, \Theta_Y, \Theta_X, \Theta_U)$ in any environment. We shall assume that environments are randomly sampled from a *distribution over mechanisms* by defining non-degenerate probability measures for each causal mechanism.

Assumption 4 (Non-degenerate Probabilistic Independent Causal Mechanisms). *The independent causal mechanisms are non-degenerate random variables with probability measures $P(\Theta_V)$ for all $V \in \{T, Y, X, U\}$ such that $\Theta_T, \Theta_Y, \Theta_X$ and Θ_U are pairwise independent random variables.*

With the above assumption, when we now say *independent* causal mechanisms, we refer to statistical independence between them. We argue that the above assumption is not particularly strong if we already have Assumption 3; the mechanisms are now allowed to change across environments in a probabilistic manner. Guo et al. (2022) proved the existence of such probability measures for the causal mechanisms when the data comprises an infinitely exchangeable sequence of random variables subject, drawing parallels to de Finetti’s theorem (de Finetti, 1937).

Hierarchical model of the environments Using these assumptions, we can now express the distribution of the datasets $\{D_k\}_{k=1}^K$ as a hierarchical model (Gelman et al., 2013, Chapter 5), wherein we first sample the mechanisms i.i.d. $\Theta_V^{(k)} \sim P(\Theta_V)$ for $k = 1, \dots, K$ and $V \in \{T, Y, X, U\}$ and then, for each environment k , obtain $(T_i^{(k)}, Y_i^{(k)}, X_i^{(k)}, U_i^{(k)})$ by repeatedly sampling N_k times according to (2). Using plate notation, we can compactly represent this hierarchical model in the augmented DAG \mathcal{G}^* shown in Figure 1a. The edges in \mathcal{G}^* between $(T_i^{(k)}, Y_i^{(k)}, X_i^{(k)}, U_i^{(k)})$ are the same as those between (T, Y, X, U) in \mathcal{G} and $\Theta_V^{(k)} \in \text{Pa}(V_i^{(k)})$ where $V \in \{T, Y, X, U\}$, for all i and k .

In the next parts of the paper, we will prove how the structure of \mathcal{G}^* implies novel observable constraints in the multi-environment data distribution that can be exploited to statistically tests the presence of hidden confounding between T and Y after having adjusted for X . But first, we discuss the main literature related to our work.

3 Related work

This paper contributes to the growing body of research based on the principle of *Independent Causal Mechanisms* (Peters et al., 2017) which has inspired further research on integrating machine learning and causality (Schölkopf et al., 2012; Peters et al., 2016; von Kügelgen et al., 2020; Schölkopf et al., 2021). Multiple works have demonstrated how the independent causal mechanism principle could improve causal structure learning when data comes from heterogeneous environments that share the same causal model (Zhang et al., 2017; Ghassami et al., 2018; Guo et al., 2022). In particular, Guo et al. (2022) demonstrated how independent causal mechanisms imply independence constraints similar to ours when the data is exchangeable – but they assume there exist no unobserved latent variables in contrast to our work where we detect the presence of such variables.

Detecting hidden confounding is hard, and often we can only reason about the plausibility of having unmeasured confounders using some sort of sensitivity analysis (Rosenbaum and Rubin, 1983a; VanderWeele and Ding, 2017; Cinelli et al., 2019). Other approaches check whether a treatment effect estimate is robust to changes in our assumptions by varying the adjustment set (Lu and White, 2014; Oster, 2019; Su and Henckel, 2022). However, the guarantees are elusive for whether this type of robustness implies unconfoundedness. Similarly, one could test for heterogeneity of the treatment effect estimates from multiple environments and conclude that if they are different, then it is due to unobserved confounding; this idea bears resemblance to the pseudo-treatment approach discussed by Imbens and Rubin (2015) for assessing unconfoundedness. But testing heterogeneity to detect confounding only works if the treatment effect is assumed to be fixed across all environments, which excludes many real-world settings. Lastly, Janzing and Schölkopf (2018) proposed a method to detect hidden confounding which is restricted to settings with linear models.

In the setting with data from multiple environments, various approaches have been proposed to deal with hidden confounding, typically by combining both experimental and observational data (Bareinboim and Pearl, 2016; Kallus et al., 2018; Athey et al., 2020; Hatt et al., 2022; Ilse et al., 2022; Imbens et al., 2022). In contrast, we consider a setting

combining *only* observational data from multiple environments. Here, the principled *Joint Causal Inference* (JCI) framework (Mooij et al., 2020) is suitable; it demonstrates how to apply traditional constraint-based methods for causal discovery (Glymour et al., 2019) with multi-environment data. In the simpler setting with observed variables (T, Y, E) excluding X , the JCI framework informs us that $Y \perp\!\!\!\perp_P E \mid T$ is violated in the presence of a hidden confounder U if E is an instrumental variable. But this means, once again, that the treatment effect is fixed across environments as we assume E has no direct effect on Y . Variants of this type of test have also been mentioned by others, for instance Athey et al. (2020, Lemma 3) and Dahabreh et al. (2020). We demonstrate the limitations of using this approach in our experiments, and provide a more in-depth explanation using graph-based arguments in Appendix C. Our contribution is a more general non-parametric test that works even if E is an invalid instrument that can influence any of the other variables.

4 Detecting hidden confounding in multi-environment data

Our goal is to detect the presence of hidden confounding between treatment T and outcome Y after having adjusted for some observed confounders X . Graphically, this corresponds to detecting the existence of both edges $U \rightarrow T$ and $U \rightarrow Y$ in the causal DAG \mathcal{G} . In this section, we demonstrate testable conditional independencies between the observed variables that are *only* violated when both those edges exist – hence providing testable implications for hidden confounding.

While we do not assume to know the complete causal DAG \mathcal{G} between our variables, we put two restrictions on it: (i) that Y is not an ancestor of T and (ii) that X is a confounder to both T and Y in contrast to, for instance, being a mediator or only a cause to either one of them. These restrictions are relatively weak as (i) holds in all practical causal inference settings as a treatment T happens before outcome Y in time and (ii) can sometimes be verified by checking that both T and Y depend on X . Under this setting, we prove the following.

Theorem 1. *Let $\mathbf{T}^{(k)} = (T_1^{(k)}, \dots, T_{N_k}^{(k)})$ be the vector of all observed treatments in environments $E^{(k)}$; define $\mathbf{Y}^{(k)}$, $\mathbf{X}^{(k)}$, and $\mathbf{U}^{(k)}$ similarly. We consider the data distribution $P(\mathbf{T}^{(k)}, \mathbf{Y}^{(k)}, \mathbf{X}^{(k)}, \mathbf{U}^{(k)})$ with $N_k \geq 2$ under assumption 1, 2, 3 and 4. Furthermore, assume an underlying causal DAG \mathcal{G} where Y is not an ancestor of T , and that X is a known common cause to T and Y . Then, for any $k = 1, \dots, K$, there exists hidden confounding between T and Y in \mathcal{G} if and only if*

$$T_j^{(k)} \not\perp\!\!\!\perp_P Y_i^{(k)} \mid T_i^{(k)}, X_i^{(k)}, X_j^{(k)} \quad \forall i, j = 1, \dots, N_k : i \neq j. \quad (3)$$

Proof sketch. To prove the statement, we look at d-separations in the extended causal graphical model \mathcal{G}^* and show that (3) only is true for corresponding graphs \mathcal{G} where the unobserved U is a confounder between T and Y . Figure 1b illustrates how open paths may exist between pairs of observations (i, j) going through $\Theta_T^{(k)}$, $\Theta_Y^{(k)}$, $\Theta_X^{(k)}$ or $\Theta_U^{(k)}$ by unrolling the augmented graph \mathcal{G}^* . These paths are open because of Assumption 4. This technique resembles the twin network method used for counterfactual inference (Balke and Pearl, 1994) but the results we obtain from using this approach are distinctly different. The complete proof can be found in the Appendix. \square

The variables $T_j^{(k)}$ and $Y_i^{(k)}$ are the treatment and outcome of two different observations in the same environment. Intuitively, the theorem states that after having adjusted for $(T_i^{(k)}, X_i^{(k)}, X_j^{(k)})$, we would expect under the ICM principle that $T_j^{(k)}$ to not provide any information about how $Y_i^{(k)}$ behaves. Thus, if it still does, then this can only be due to unobserved confounding. Testing this independence hence provides us with a testable implication in our observed data distribution on whether the unobserved U is a confounder or not.

Two-variable case without observed confounders We can drop the observed confounder X in Theorem 1 and, interestingly, in that case, obtain even stronger results for detecting the presence of a hidden confounder. This setting is interesting as even the two-variable case is notoriously difficult in causal discovery (Reichenbach, 1956; Peters et al., 2017). Unlike in the more general setting, we no longer need to know the direction of the causal relationship between T and Y .

Theorem 2. *Let $\mathbf{T}^{(k)} = (T_1^{(k)}, \dots, T_{N_k}^{(k)})$ be the vector of all observed treatments in environments $E^{(k)}$; define $\mathbf{Y}^{(k)}$ and $\mathbf{U}^{(k)}$ similarly. We consider the data distribution $P(\mathbf{T}^{(k)}, \mathbf{Y}^{(k)}, \mathbf{U}^{(k)})$ without any observed confounders and*

$N_k \geq 2$ under assumption 1, 2, 3 and 4. Then, for any $k = 1, \dots, K$, there exists hidden confounding between T and Y in \mathcal{G} if and only if

$$(i) \quad T_j^{(k)} \not\perp_P Y_i^{(k)} \mid T_i^{(k)} \quad \text{and} \quad (ii) \quad T_j^{(k)} \not\perp_P Y_i^{(k)} \mid Y_j^{(k)} \quad \forall i, j = 1, \dots, N_k : i \neq j. \quad (4)$$

Guo et al. (2022) studied a similar setting to Theorem 2 and demonstrated how to decide the causal direction between T and Y in this case when there is no latent variable. Our results extend theirs as we now also show how to exclude the possibility of a latent common cause in this setting. The proof is similar to that of Theorem 1, but the conditional independencies are different. Firstly, we have $T_j^{(k)} \not\perp_P Y_i^{(k)} \mid T_i^{(k)}$ which is the conditional independence in Theorem 1 without conditioning on $X_i^{(k)}$ and $X_j^{(k)}$. Secondly, we have $T_j^{(k)} \not\perp_P Y_i^{(k)} \mid Y_j^{(k)}$. This one is necessary as we no longer assume anything about the ancestral relationship between treatment and outcome. If we had assumed that T could not be a descendant of Y , we can show that only condition (i) in the theorem is necessary. Similarly, condition (ii) is only necessary when Y could not be a descendant of T .

4.1 Influence of the assumptions

Our theory shows how to test for hidden confounding, but it now relies on other untestable assumptions: namely non-degenerate independent causal mechanisms and the faithfulness & causal Markov property. Due to this, we investigate the necessity of these assumptions and identify various failure cases when they are violated. On a more positive note, we also demonstrate that the assumption of non-degenerate mechanisms can be weakened. We present here the main conclusions regarding violations on two of the assumptions while more elaborate explanations can be found in Appendix E together with a demonstration of how our procedure can fail due to faithfulness violations in linear-Gaussian structural causal models.

Violation of Assumption 3: dependent causal mechanisms What happens if any of the pair-wise independencies between $\Theta_T, \Theta_Y, \Theta_X$ or Θ_U are violated? To investigate this, we go through the same procedure for proving Theorem 1 where we allow any of these mechanisms to be dependent. We find that $T_j^{(k)} \not\perp_P Y_i^{(k)} \mid T_i^{(k)}, X_i^{(k)}, X_j^{(k)}$ can be violated even when there is no confounding in all but one case with dependent mechanisms, meaning that it no longer works for detecting hidden confounding. The only case where our theory still works is when $\Theta_X \not\perp_P \Theta_U$ – i.e. the mechanisms of the observed and unobserved confounders are allowed to co-vary across environments.

Violation of Assumption 4: degenerate causal mechanisms What happens if one or more of the distributions $P(\Theta_T), P(\Theta_Y), P(\Theta_X)$ and $P(\Theta_U)$ are degenerate, meaning that some mechanisms are fixed across all environments? In the most extreme case, if all mechanisms are fixed then the distribution P_E would be identical in each environment. We investigate these scenarios by first adding $\Theta_T, \Theta_Y, \Theta_X$ and/or Θ_U to the conditioning set of the independence in Theorem 1. Then, we check whether this independence still is violated in the presence of hidden confounding using the same procedure used for proving the theorem. We find that the theorem fails only when we condition on both Θ_T and Θ_U . In other words, it is only strictly necessary for our theory that changes in $P_{\Theta_T}(T \mid \text{Pa}(T))$ or $P_{\Theta_U}(U \mid \text{Pa}(U))$ occur between environments.

Remark 1. We may now identify a more conservative interpretation of our proposed procedure. First, one can verify the assumption of non-degenerate causal mechanisms by checking from data whether $P_E(T \mid X)$ varies across environments; if it does, then that is likely because Θ_T and/or – through potential downstream effects – Θ_U are non-degenerate. Next, we would run our proposed procedure. Now if the null is rejected then we can be conservative by concluding that this is either because we have hidden confounding and/or dependent mechanisms. But in the case of no rejection, it can only be interpreted as having no hidden confounders present. This is because having dependent causal mechanisms (violation of assumption 3) can only cause false positives.

4.2 Testing the independence

Here, we explain how test the conditional independence $T_j^{(k)} \not\perp_P Y_i^{(k)} \mid T_i^{(k)}, X_i^{(k)}, X_j^{(k)}$ from Theorem 1 using multi-environment data; the full procedure is summarized in Algorithm 1 in the Appendix. To test this independence, we need to simulate sampling from the joint distribution $P(T_i^{(k)}, Y_i^{(k)}, X_i^{(k)}, T_j^{(k)}, Y_j^{(k)}, X_j^{(k)})$, note here that we do not condition on $E^{(k)}$. The idea is as follows: we select two different observations i and j from all environments such

that we get a vector of observed treatments $t_i = (t_i^{(1)}, t_i^{(2)}, \dots, t_i^{(K)})$; outcomes $y_i = (y_i^{(1)}, y_i^{(2)}, \dots, y_i^{(K)})$; and so on for x_i, t_j and x_j . Then, we can use any suitable method for conditional independence testing with t_i, y_i, x_i, t_j and x_j . Note that choice of observations within each environment is arbitrary as long as we do not pick the same observation for i and j , this is a consequence of observations being i.i.d. within each environment.

Increasing power of test with Fisher’s method In essence, we perform a conditional independence test where the “sample size” of the test is the number of available environments. Thus, for a small number of environments, our test might have low power (probability of detecting hidden confounding when it is present). To alleviate this issue, we recognize that we can perform this test multiple times if we have many samples N_k per environment. Then, we would select new observations from every environment for each hypothesis test until all observations have been used up. Note that the number of samples N_k might change per environment, so we only select from environments where there still are observations that have not yet been used for the hypothesis testing. Since each hypothesis test is independent and has the same null, we can aggregate the p-values from all tests using Fisher’s method to obtain a global hypothesis test (Fisher, 1925). As we show in our experiments, this drastically improves the power of our method, thus reducing the number of environments needed to detect the presence of hidden confounding.

5 Experiments

To evaluate and investigate the theory for testing hidden confounding in multi-environment data, we perform a series of simulation studies with synthetic data in addition to experiments with semi-synthetic data generated using the Twins dataset (Almond et al., 2005; Louizos et al., 2017). As we want to evaluate our method’s ability to detect confounding, we use data where the ground-truth causal graph is known. The experiments are implemented in Python.² Unless otherwise stated, each experiment is repeated 50 times where we use a significance level $\alpha = 0.05$. Depending on the variable types in the experiment, we state what suitable conditional independence testing method is used by our algorithm.

5.1 Synthetic data

For the synthetic data experiments, we generate data as follows: we have the confounder $U_i^{(k)} \sim \text{Normal}(\Theta_U^{(k)}, 1)$; treatment $T_i^{(k)} \sim \text{Ber}(\text{Sigm}(U_i^{(k)} + \Theta_T^{(k)}))$; and outcome $Y_i^{(k)} \sim \text{Ber}(\text{Sigm}(\lambda U_i^{(k)} + T_i^{(k)} + \Theta_Y^{(k)}))$. Note $\text{Sigm}(x) = 1/(1 + e^{-x})$ is the logistic function and $\Theta_V^{(k)} \sim \text{Normal}(0, \sigma_{\Theta_V}^2)$ for $V \in \{T, Y, U\}$. Unless otherwise stated, we use $\sigma_{\Theta_T} = \sigma_{\Theta_U} = \sigma_{\Theta_Y} = 1$. We control the strength of confounding by varying λ , where $\lambda = 0$ corresponds to no confounding.

Larger confounder effect sizes increase the probability of detection We investigate how the effect size of the confounding variable influences our proposed testing procedure. We vary λ between 0 (no confounding) and 10 while also varying the number of environments. We perform this experiment with $N_k = 2$ for all k and use the G-test for conditional independence testing (McDonald, 2014). The results are shown in Figure 3a. We note two things: the probability of detection grows for larger confounder effect size and it also grows when the number of environments is increased.

The growth rate in detection depends on the number of environments We investigate the probability of detecting confounding when varying both the number of environments and the number of samples per environment for a fixed confounding strength $\lambda = 5$. We use a permutation-based method for the conditional independence test (Tsamardinos and Borboudakis, 2010) as we do not want to rely only on asymptotic validity (such as in the G-test) due to the limited number of environments. The results show that the performance of the testing procedure is highly dependent on the number of environments K , see 3b. The probability of detection grows as we increase the number of samples. Noticeably, the rate of growth increases with the number of environments K .

Robustness to environmental changes We compare our proposed procedure to the alternative approach of testing $Y \perp_P E \mid T$ to detect hidden confounding, the latter being valid when E is an instrumental variable (Mooij et al.,

²Code available at github.com/RickardKarl/detect-hidden-confounding.

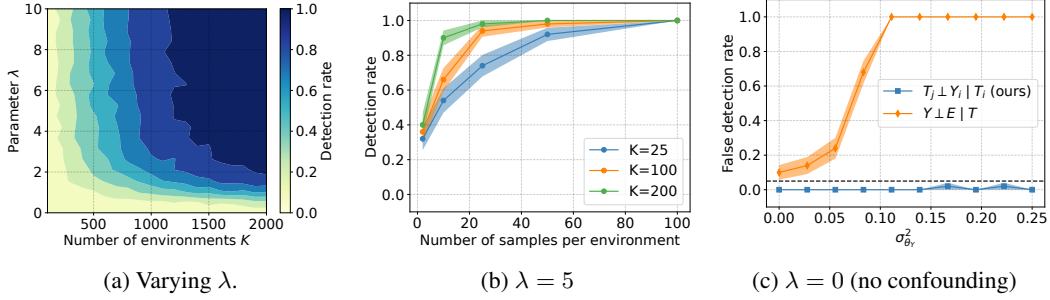


Figure 3: **Synthetic data** – (a): Detecting confounding with $N_k = 2$ across a range of confounder effect sizes and numbers of environments K . (500 repetitions) (b): Simulations with fixed confounding strength $\lambda = 5$ for $N_k > 2$ with a small number of environments K . (c): Comparing the proposed procedure and an alternative testing procedure by varying the standard deviation of Θ_Y in the absence of confounding. The black dashed line corresponds to the desired type 1 error control $\alpha = 0.05$. The shaded area shows the standard error from 50 repetitions.

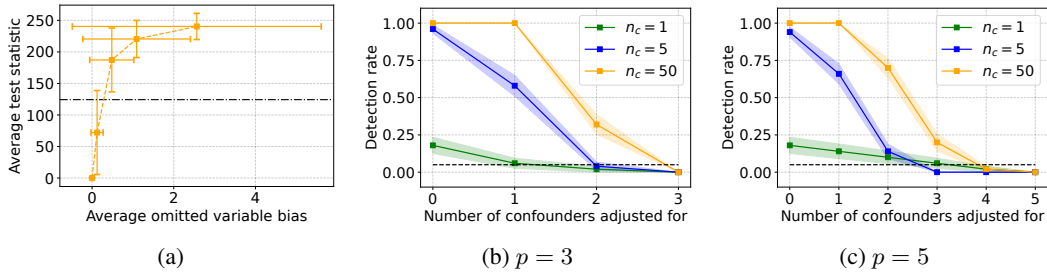


Figure 4: **Twins dataset** – (a): Effect of bias from omitting confounders on the test statistic of our hypothesis test. (b), (c): Performance when adjusting for observed confounders with either a total of 3 or 5 confounders in the data. The different curves correspond to combining numbers of hypothesis tests. The black dashed line corresponds to the rejection threshold / desired type 1 error $\alpha = 0.05$ in all figures, and the error bars / shaded area shows standard deviation (figure a) or standard error (figure b and c) from 50 repetitions.

2020). Here we test the sensitivity to violating one of its conditions, namely that $P_E(Y | T)$ is fixed under the null. We vary σ_{Θ_Y} between 0 and $\frac{1}{4}$ when there is no confounding by setting $\lambda = 0$ with $N = 100$ and $K = 500$, and we use the G-test for conditional independence testing (McDonald, 2014). As shown in Figure 3c, the probability of false detection using $Y \perp_P E | T$ increases when σ_{Θ_Y} starts to increase. Meanwhile, the false detection rate (type 1 error) remains bounded by $\alpha = 0.05$ for our procedure as desired. In Appendix G, we also include the same comparison when confounding is present to confirm that our method is able to detect confounding in this case.

5.2 Twins dataset

We use data from twin births in the USA between 1989-1991 (Almond et al., 2005; Louizos et al., 2017) to construct an observational dataset with continuous treatment/outcome and non-linear relationships. Here the environments are different states, and a notable element of our dataset is that all variations between environments stem solely from the real-world distribution shifts of the covariates between birth states. The strength of confounding is controlled by a parameter λ , where $\lambda = 0$ corresponds to no confounding. The full procedure for data generation is described in Appendix F. For the following experiments, we use the Kernel Conditional Independence Test (Zhang et al., 2012) in our algorithm due to having continuous variables and, unless otherwise stated, combine 50 hypothesis tests using Fisher’s method.

Detection rate increases with bias from unobserved confounding We perform an experiment having $p = 5$ unobserved confounders, where we vary confounding strength λ between 0 and 5. We compute the bias from omitting the unobserved confounders when estimating the average treatment effect of T on Y in each environment. We then compare the average bias to the test statistic computed by our algorithm averaged over multiple iterations. As observed

in Figure 4a, the test statistic increases together with the bias. The black dashed line in the figure represents the rejection threshold at $\alpha = 0.05$, hence we can see that for sufficient bias the method will detect it.

Adjusting for observed confounders In the last experiments, we attempt to detect hidden confounding while also adjusting for observed confounders. We go from observing none to all confounders while having a confounding strength of $\lambda = 5$. We do this for the case with either a total of $p = 3$ or $p = 5$ confounders, shown in Figure 4b and 4c, respectively. In addition, we investigate the influence of combining multiple hypothesis tests (n_c denotes the number of tests) using Fisher’s method. We observe first that adjusting for more confounders leads to a decrease in detection rate, and that our desired type 1 error of $\alpha = 0.05$ is controlled when we have adjusted for all confounders. Secondly, the performance deteriorates when the total number of confounders increases, as indicated by the detection rate, which is lower when adjusting for 4 confounders when $p = 5$ than adjusting for 2 confounders when $p = 3$. This is likely because the conditional independence test loses power as the conditioning set becomes larger (Zhang et al., 2012). Thirdly, we see that the combination of multiple hypothesis tests using Fisher’s method does improve the power of our algorithm. We did, however, not see any significant benefit in combining more than 50 hypothesis tests in these experiments.

6 Discussion

In this work, we studied a setting where observational data has been collected from different heterogeneous environments in which the same treatment T , outcome Y , and covariates X have been observed. We showed that, assuming independent causal mechanisms, there exist testable conditional independencies that are violated in the presence of hidden confounders, for which we also proposed a statistical procedure to test these independencies from observed data. In many cases, with a sufficient number of environments, we show that we are able to detect confounding when it is present. While our main goal was to derive testable implications of hidden confounding, open questions remain on how to improve sample efficiency and tackle loss of power when adjusting for many observed confounders. Addressing these can lead to better tools for researchers to validate their causal assumptions and move towards doing safer causal inference.

Acknowledgements

The authors thank Marco Loog, Stephan Bongers, other members of the Pattern Recognition lab, Alexander Mey and Frans Oliehoek for their valuable feedback on earlier versions of this manuscript.

References

- Judea Pearl. *Causality*. Cambridge University Press, 2nd edition, 2009.
- Jonas Peters, Dominik Janzing, and Bernhard Schölkopf. *Elements of Causal Inference: Foundations and Learning Algorithms*. MIT Press, 1st edition, 2017.
- Bernhard Schölkopf, Francesco Locatello, Stefan Bauer, Nan Rosemary Ke, Nal Kalchbrenner, Anirudh Goyal, and Yoshua Bengio. Toward causal representation learning. *Proceedings of the IEEE*, 109(5):612–634, 2021.
- Monika Mueller, Maddalena D’Addario, Matthias Egger, Myriam Cevallos, Olaf Dekkers, Catrina Mugglin, and Pippa Scott. Methods to systematically review and meta-analyse observational studies: a systematic scoping review of recommendations. *BMC medical research methodology*, 18(1):1–18, 2018.
- Douglas Almond, Kenneth Y Chay, and David S Lee. The costs of low birth weight. *The Quarterly Journal of Economics*, 120(3):1031–1083, 2005.
- Christos Louizos, Uri Shalit, Joris M Mooij, David Sontag, Richard Zemel, and Max Welling. Causal effect inference with deep latent-variable models. *Advances in neural information processing systems*, 30, 2017.
- Judea Pearl. *Probabilistic reasoning in intelligent systems: networks of plausible inference*. Morgan kaufmann, 1988.
- Joshua D Angrist, Guido W Imbens, and Donald B Rubin. Identification of causal effects using instrumental variables. *Journal of the American statistical Association*, 91(434):444–455, 1996.
- Dominik Janzing and Bernhard Schölkopf. Causal inference using the algorithmic markov condition. *IEEE Trans. Inf. Theor.*, 56(10):5168–5194, 2010. ISSN 0018-9448.

- Siyan Guo, Viktor Tóth, Bernhard Schölkopf, and Ferenc Huszár. Causal de Finetti: On the Identification of Invariant Causal Structure in Exchangeable Data. arXiv preprint arXiv:2203.15756, 2022.
- Bernhard Schölkopf, Dominik Janzing, Jonas Peters, Eleni Sgouritsa, Kun Zhang, and Joris Mooij. On causal and anticausal learning. In Proceedings of the 29th International Conference on Machine Learning, page 459–466. Omnipress, 2012. ISBN 9781450312851.
- Bruno de Finetti. La prévision : ses lois logiques, ses sources subjectives. Annales de l’institut Henri Poincaré, 7(1): 1–68, 1937.
- Andrew Gelman, John B Carlin, Hal S Stern, David B Dunson, Aki Vehtari, and Donald B Rubin. Bayesian data analysis. CRC press, 2013.
- Jonas Peters, Peter Bühlmann, and Nicolai Meinshausen. Causal inference by using invariant prediction: identification and confidence intervals. Journal of the Royal Statistical Society: Series B (Statistical Methodology), 78(5):947–1012, 2016.
- Julius von Kügelgen, Alexander Mey, Marco Loog, and Bernhard Schölkopf. Semi-supervised learning, causality, and the conditional cluster assumption. In Proceedings of the 36th Conference on Uncertainty in Artificial Intelligence (UAI), volume 124, pages 1–10. PMLR, 2020.
- Kun Zhang, Biwei Huang, Jiji Zhang, Clark Glymour, and Bernhard Schölkopf. Causal discovery from nonstationary/heterogeneous data: Skeleton estimation and orientation determination. In Proceedings of the Twenty-Sixth International Joint Conference on Artificial Intelligence, IJCAI-17, pages 1347–1353, 2017.
- AmirEmad Ghassami, Negar Kiyavash, Biwei Huang, and Kun Zhang. Multi-domain causal structure learning in linear systems. Advances in neural information processing systems, 31, 2018.
- P. R. Rosenbaum and D. B. Rubin. Assessing sensitivity to an unobserved binary covariate in an observational study with binary outcome. Journal of the Royal Statistical Society. Series B (Methodological), 45(2):212–218, 1983a. ISSN 00359246.
- Tyler J VanderWeele and Peng Ding. Sensitivity analysis in observational research: introducing the e-value. Annals of internal medicine, 167(4):268–274, 2017.
- Carlos Cinelli, Daniel Kumor, Bryant Chen, Judea Pearl, and Elias Bareinboim. Sensitivity analysis of linear structural causal models. In International conference on machine learning, pages 1252–1261. PMLR, 2019.
- Xun Lu and Halbert White. Robustness checks and robustness tests in applied economics. Journal of econometrics, 178:194–206, 2014.
- Emily Oster. Unobservable selection and coefficient stability: Theory and evidence. Journal of Business & Economic Statistics, 37(2):187–204, 2019.
- Zehao Su and Leonard Henckel. A robustness test for estimating total effects with covariate adjustment. In The 38th Conference on Uncertainty in Artificial Intelligence, 2022.
- Guido W Imbens and Donald B Rubin. Causal inference in statistics, social, and biomedical sciences. Cambridge University Press, 2015.
- Dominik Janzing and Bernhard Schölkopf. Detecting confounding in multivariate linear models via spectral analysis. Journal of Causal Inference, 6(1):20170013, 2018. doi: doi:10.1515/jci-2017-0013.
- Elias Bareinboim and Judea Pearl. Causal inference and the data-fusion problem. Proceedings of the National Academy of Sciences, 113(27):7345–7352, 2016.
- Nathan Kallus, Aahlad Manas Puli, and Uri Shalit. Removing Hidden Confounding by Experimental Grounding. In Advances in Neural Information Processing Systems, volume 31. Curran Associates, Inc., 2018.
- Susan Athey, Raj Chetty, and Guido Imbens. Combining Experimental and Observational Data to Estimate Treatment Effects on Long Term Outcomes. arXiv preprint arXiv:2006.09676, 2020.
- Tobias Hatt, Jeroen Berrevoets, Alicia Curth, Stefan Feuerriegel, and Mihaela van der Schaar. Combining Observational and Randomized Data for Estimating Heterogeneous Treatment Effects. arXiv preprint arXiv:2202.12891, 2022.
- Maximilian Ilse, Patrick Forré, Max Welling, and Joris M. Mooij. Combining Interventional and Observational Data Using Causal Reductions. arXiv preprint arXiv:2103.04786, 2022.
- Guido Imbens, Nathan Kallus, Xiaojie Mao, and Yuhao Wang. Long-term Causal Inference Under Persistent Confounding via Data Combination. arXiv preprint arXiv:2202.07234, 2022.
- Joris M. Mooij, Sara Magliacane, and Tom Claassen. Joint causal inference from multiple contexts. Journal of Machine Learning Research, 21(99):1–108, 2020.

- Clark Glymour, Kun Zhang, and Peter Spirtes. Review of causal discovery methods based on graphical models. *Frontiers in Genetics*, 10, 2019. ISSN 1664-8021.
- Issa J Dahabreh, James M Robins, and Miguel A Hernán. Benchmarking observational methods by comparing randomized trials and their emulations. *Epidemiology (Cambridge, Mass.)*, 31(5):614–619, 2020.
- Alexander Balke and Judea Pearl. Counterfactual probabilities: Computational methods, bounds and applications. In *Uncertainty Proceedings 1994*, pages 46–54. Elsevier, 1994.
- Hans Reichenbach. *The Direction of Time*. Dover Publications, 1956.
- Ronald A Fisher. *Statistical Methods for Research Workers*. Oliver and Boyd, 1925.
- John H. McDonald. *Handbook of Biological Statistics*. Sparky House Publishing, 3rd edition, 2014.
- Ioannis Tsamardinos and Giorgos Borboudakis. Permutation testing improves bayesian network learning. In José Luis Balcázar, Francesco Bonchi, Aristides Gionis, and Michèle Sebag, editors, *Machine Learning and Knowledge Discovery in Databases*, pages 322–337, Berlin, Heidelberg, 2010. Springer Berlin Heidelberg.
- Kun Zhang, Jonas Peters, Dominik Janzing, and Bernhard Schölkopf. Kernel-based conditional independence test and application in causal discovery. *arXiv preprint arXiv:1202.3775*, 2012.
- Manabu Kuroki and Judea Pearl. Measurement bias and effect restoration in causal inference. *Biometrika*, 101(2): 423–437, 2014. ISSN 0006-3444.
- Wang Miao, Zhi Geng, and Eric J Tchetgen Tchetgen. Identifying causal effects with proxy variables of an unmeasured confounder. *Biometrika*, 105(4):987–993, 2018. ISSN 0006-3444.
- Edwin P Martens, Wiebe R Pestman, Anthonius de Boer, Svetlana V Belitser, and Olaf H Klungel. Instrumental variables: application and limitations. *Epidemiology*, pages 260–267, 2006.
- Paul R Rosenbaum and Donald B Rubin. The central role of the propensity score in observational studies for causal effects. *Biometrika*, 70(1):41–55, 1983b.
- Johannes Textor, Benito van der Zander, Mark S Gilthorpe, Maciej Liśkiewicz, and George TH Ellison. Robust causal inference using directed acyclic graphs: the R package ‘dagitty’. *International Journal of Epidemiology*, 45(6): 1887–1894, 2017.
- Christopher Meek. Strong completeness and faithfulness in bayesian networks. In *Proceedings of the Eleventh Conference on Uncertainty in Artificial Intelligence, UAI’95*, page 411–418, San Francisco, CA, USA, 1995. Morgan Kaufmann Publishers Inc. ISBN 1558603859.
- Kunihiro Baba, Ritei Shibata, and Masaaki Sibuya. Partial correlation and conditional correlation as measures of conditional independence. *Australian & New Zealand Journal of Statistics*, 46(4):657–664, 2004.

Appendix

The appendix contains the following sections.

- A. **Future Work:** This section contains a discussion on open questions that we have identified in this work.
- B. **Proofs:** This section provides the full proof of Theorem 1 and 2.
- C. **Alternative Test for Detecting Hidden Confounding in Two-variable Case:** We discuss the alternative approach of testing $Y \perp\!\!\!\perp_P E \mid T$ to detect hidden confounding in the two-variable case without any observed confounder. We demonstrate conditions when and when not it would work.
- D. **Our Algorithm:** We provide the pseudo-code for our algorithm that statistically tests the presence of hidden confounding from multi-environment data.
- E. **Further Analysis on the Influence of the Assumptions:** We elaborate on the examples of violating the assumptions behind our theory, as discussed in Section 4.1. First, we provide concrete failure cases when we have dependent causal mechanisms. Secondly, we demonstrate how we can relax the assumptions on non-degenerate mechanisms. Finally, we give also give an example of faithfulness violations in linear-Gaussian structural causal models.
- F. **Generation of Twins Semi-synthetic Dataset:** We explain how to generate the semi-synthetic observational data using the Twins dataset.
- G. **Additional Experiments:** We perform additional simulation studies, extending the results in the main paper with results with both continuous and binary data.

A Future Work

We have identified a set of open questions deriving from our work. Firstly, our theory applies to the common setting in causal inference with treatment T , outcome Y and a possibly high-dimensional confounder X , in which we want to detect the presence of additional hidden confounding U (that also can be high-dimensional). While this is arguably the most typical setting in causal inference, it is of interest to consider other scenarios with more variables and interactions between them. We conjecture that other testable implications exist for confounding in these settings that could be found with similar arguments as we use. A particularly interesting setting is when we observe a proxy to a hidden confounder, which can be used for adjustment instead (Kuroki and Pearl, 2014; Miao et al., 2018). In this case, it is no longer straightforward to say whether there could be a hidden confounder which is unrelated to the proxy. We also believe that our techniques might be applicable to scenarios with instrumental variables (IV) (Angrist et al., 1996; Martens et al., 2006), to test whether there exists any confounding between the IV and treatment which is a requirement for valid IV estimation.

Secondly, our theorem fundamentally relies on a set of untestable assumptions: independent & non-degenerate causal mechanisms and the faithfulness & causal Markov property. Although we investigated various violations, these results raised new questions. In particular, the effect of faithfulness violations, perhaps surprisingly, had a large influence on our procedure. Therefore, it is important to understand whether similar observations can be made in more realistic settings.

Thirdly, an interesting direction for future research would be to investigate how our approach can be used to estimate confounding strength, to be used in well-studied approaches in sensitivity analysis (Rosenbaum and Rubin, 1983a; Cinelli et al., 2019).

Lastly, while our main goal was to derive testable implications of hidden confounding, there are opportunities to improve the way we test these from data. We observed that our proposed procedure sometimes requires a large number of environments. While it is unclear whether this is a property of the theory or the lack of efficiency in the test procedure we used, we note that combining multiple hypothesis tests using Fisher’s method helped with performance. A possible research direction could be to investigate how to refine this approach further. Further, we observed performance deteriorating as we adjusted for more observed confounders, likely due to the curse of dimensionality (Zhang et al., 2012). A promising solution here could be to use popular dimensionality-reduction techniques from causal inference such as the propensity score (Rosenbaum and Rubin, 1983b).

B Proofs

In this section, we present the proof for Theorem 1 and 2. Let $\mathbf{T}^{(k)} = (T_1^{(k)}, \dots, T_{N_k}^{(k)})$ be the vector of all observed treatments in environments $E^{(k)}$. Define $\mathbf{Y}^{(k)}$, $\mathbf{X}^{(k)}$, and $\mathbf{U}^{(k)}$ similarly.

Theorem 1. *We consider the data distribution $P(\mathbf{T}^{(k)}, \mathbf{Y}^{(k)}, \mathbf{X}^{(k)}, \mathbf{U}^{(k)})$ with $N_k \geq 2$ under assumption 1, 2, 3 and 4. Furthermore, assume an underlying causal DAG \mathcal{G} where Y is not an ancestor of T , and that X is a known common cause to T and Y . Then, for any $k = 1, \dots, K$, there exists hidden confounding between T and Y in \mathcal{G} if and only if*

$$T_j^{(k)} \not\perp_P Y_i^{(k)} \mid T_i^{(k)}, X_i^{(k)}, X_j^{(k)} \quad \forall i, j = 1, \dots, N_k : i \neq j. \quad (5)$$

Proof. We constrain ourselves to DAGs \mathcal{G} with variables (T, Y, X, U) where X is a known common cause to both T and Y , and Y is not an ancestor of T in \mathcal{G} . Under the assumption of non-degenerate, independent causal mechanisms (Assumption 3 and 4), we can introduce the mechanisms Θ_V for each variable $V \in \{T, Y, X, U\}$. Further, we can augment \mathcal{G} with a hierarchical structure (Gelman et al., 2013, Chapter 5), wherein we first sample the mechanisms i.i.d. $\Theta_V^{(k)} \sim P(\Theta_V)$ for $k = 1, \dots, K$ and $V \in \{T, Y, X, U\}$ and then, for each environment k , obtain $(T_i^{(k)}, Y_i^{(k)}, X_i^{(k)}, U_i^{(k)})$ by repeatedly sampling N_k times conditioned on the mechanisms. We denote this augmented graph with the hierarchical structure as \mathcal{G}^* , where edges between $(T_i^{(k)}, Y_i^{(k)}, X_i^{(k)}, U_i^{(k)})$ are the same as for (T, Y, X, U) and $\Theta_V^{(k)} \in \text{Pa}(V_i^{(k)})$ where $V \in \{T, Y, X, U\}$, for all i and k . An example of such an augmented graph \mathcal{G}^* is shown in Figure 5. Notably, this augmentation can be done for all k because we assume that all environments share the same causal graph \mathcal{G} (Assumption 2).

Now, given the constraints that we have defined, we consider every combination of the edges between (T, Y, X, U) that are DAGs. In total, there are 40 different DAGs that encompass all these combinations of edges. We say that U

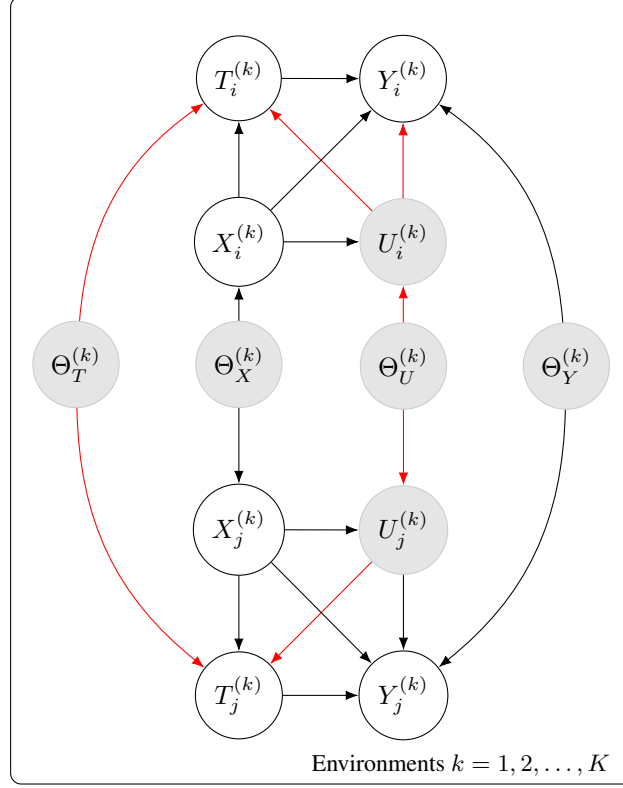


Figure 5: Example of unrolling the augmented causal DAG \mathcal{G}^* for some pair of observations (i, j) . The samples are generally not independent due to the shared mechanisms $(\Theta_T, \Theta_X, \Theta_U, \Theta_Y)$, unless we condition on them. Confounding is present, and the red edges mark open paths such that $T_j^{(k)} \not\perp_d Y_i^{(k)} \mid T_i^{(k)}, X_i^{(k)}, X_j^{(k)}$ in this graph. Note that these paths go through the outgoing edges from $U_i^{(k)}$ to $T_i^{(k)}$ and $Y_i^{(k)}$ (and similarly for j), and that the paths are closed if either of the edges is removed.

is a confounder in one of these DAGs if both the edges $U \rightarrow T$ and $U \rightarrow Y$ exist. For each of these graphs \mathcal{G} , we shall investigate the d-separations in its augmented version \mathcal{G}^* . Notably, due to the assumption of non-degenerate mechanisms (Assumption 4), we allow open paths in \mathcal{G}^* that go through $\Theta_T^{(k)}, \Theta_Y^{(k)}, \Theta_X^{(k)}$, or $\Theta_U^{(k)}$. This means that two different observations $(T_i^{(k)}, Y_i^{(k)}, X_i^{(k)}, U_i^{(k)})$ and $(T_j^{(k)}, Y_j^{(k)}, X_j^{(k)}, U_j^{(k)})$ can be dependent when $i \neq j$ for $i, j = 1, \dots, N_k$. These paths are best illustrated by unrolling the augmented graph \mathcal{G}^* as in the example in Figure 5. However, such dependencies can only happen if we do not condition on the mechanisms (that is, the environment) as we know that the observations are sampled i.i.d. within each environment. This demonstrates the need for multiple environments, as the randomness from sampling $(\Theta_T^{(k)}, \Theta_Y^{(k)}, \Theta_X^{(k)}, \Theta_U^{(k)})$ allows us to treat them as ordinary random variables. To capture this randomness, we need to observe multiple environments though. Note that we also need $N_k \geq 2$ for $i \neq j$ to hold.

We will pay attention to a particular d-separation in \mathcal{G}^* , namely

$$T_j^{(k)} \not\perp_d Y_i^{(k)} \mid T_i^{(k)}, X_i^{(k)}, X_j^{(k)}.$$

We automatically iterate over our list of DAGs using the *dagitty* package in R (Textor et al., 2017) and check whether this d-separation holds; the results are displayed in Table 1. We note that the shaded rows in the table are the cases where U is a confounder, and these are the only cases where $T_j^{(k)} \not\perp_d Y_i^{(k)} \mid T_i^{(k)}, X_i^{(k)}, X_j^{(k)}$ is violated in \mathcal{G}^* . In other words, checking this d-separation is sufficient to determine whether U is a confounder in \mathcal{G} . Assuming the faithfulness and causal Markov property (Assumption 1), we have that:

$$T_j^{(k)} \not\perp_d Y_i^{(k)} \mid T_i^{(k)}, X_i^{(k)}, X_j^{(k)} \iff T_j^{(k)} \not\perp_P Y_i^{(k)} \mid T_i^{(k)}, X_i^{(k)}, X_j^{(k)}.$$

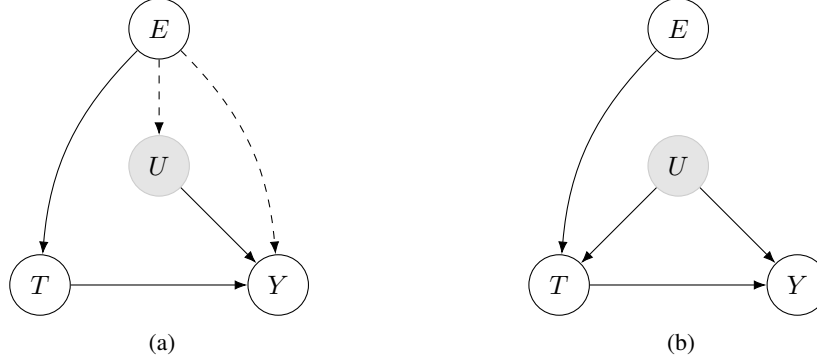


Figure 6: Examples of using $Y \perp\!\!\!\perp_P E \mid T$ to detect confounding. Gray corresponds to unobserved variables. **(a)** Violations of $Y \perp\!\!\!\perp_P E \mid T$ despite there being no confounding between T and Y . Removing the two dashed edges would make $Y \perp\!\!\!\perp_P E \mid T$ hold. **(b)** Case with correct violation of $Y \perp\!\!\!\perp_P E \mid T$ when unobserved confounding is present.

Consequently, it follows that

$$T_j^{(k)} \not\perp\!\!\!\perp_P Y_i^{(k)} \mid T_i^{(k)}, X_i^{(k)}, X_j^{(k)} \text{ for } i \neq j \iff U \text{ is a confounder to } T \text{ and } Y.$$

This results holds for any k since we assume that all environments share the same causal DAG (Assumption 2).

□

Remark 2. $X_j^{(k)}$ can be removed from the conditioning set in the independence of Theorem 1 when we assume that the observed and unobserved confounders are independent of each other. In practice, however, we most likely would not like to make this assumption which is why we recommend to condition on both $X_i^{(k)}$ and $X_j^{(k)}$.

Theorem 2. We consider the data distribution $P(\mathbf{T}^{(k)}, \mathbf{Y}^{(k)}, \mathbf{U}^{(k)})$ without any observed confounders and $N_k \geq 2$ under assumption 1, 2, 3 and 4. Then, for any $k = 1, \dots, K$, there exists hidden confounding between T and Y in \mathcal{G} if and only if

$$(i) \ T_j^{(k)} \not\perp\!\!\!\perp_P Y_i^{(k)} \mid T_i^{(k)} \text{ and } (ii) \ T_j^{(k)} \not\perp\!\!\!\perp_P Y_i^{(k)} \mid Y_j^{(k)} \ \forall i, j = 1, \dots, N_k : i \neq j. \quad (6)$$

Proof. Using the same arguments as in the proof of Theorem 1, we can show that $T_j^{(k)} \not\perp\!\!\!\perp_P Y_i^{(k)} \mid T_i^{(k)}$ and $T_j^{(k)} \not\perp\!\!\!\perp_P Y_i^{(k)} \mid Y_j^{(k)}$ exclusively holds for those where there exists no common cause between T and Y when we only have the variables (T, Y, U) , excluding any observed confounder X . The corresponding table to check this is demonstrated in Table 2. □

C Alternative Test for Detecting Hidden Confounding in Two-variable Case

In this section, we explain when (and when not) testing $Y \perp\!\!\!\perp_P E \mid T$ is a valid strategy for detecting hidden confounding between T and Y . We require that $Y \perp\!\!\!\perp_P E \mid T, U$ when there is no confounding meaning that there can not exist any direct causal relationships $E \rightarrow Y$ or $E \rightarrow U$; if this does not hold then testing $Y \perp\!\!\!\perp_P E \mid T$ would not be informative. This is demonstrated with the dashed edges in Figure 6a. Meanwhile, in Figure 6b, we display the case where a violation of $Y \perp\!\!\!\perp_P E \mid T$ correctly detects hidden confounding being present. The conclusion is that this alternative test, which is easy to test, only works if the changes between environments happen for the conditional distribution $P_E(T \mid \text{Pa}(T))$, as only T may be directly caused by E if this test shall work. This corresponds to E being an instrumental variable (Angrist et al., 1996), meaning that $T \not\perp\!\!\!\perp_P E$, $U \perp\!\!\!\perp_P E$, and the environment E can not have any direct effect on the outcome Y under the null (that is no confounding).

D Our Algorithm

To statistically test the conditional independencies presented in our theory, we present Algorithm 1 that uses any suitable conditional independence test to detect the presence of hidden confounding with data from multiple environments. The intuition for how it works is described in Sec. 4.2. Note that in the algorithm, we define $t_{2i-1}^{\pi_{2i}} := \{t_{2i-1}^{(k)}\}_{k \in \pi_{2i}}$ and similarly for $y_{2i}^{\pi_{2i}}, x_{2i}^{\pi_{2i}}, x_{2i-1}^{\pi_{2i}}$ and $x_{2i}^{\pi_{2i}}$.

Algorithm 1: Algorithm for statistically testing the presence of hidden confounding.

Input: Datasets $D_k = \{(t_i^{(k)}, y_i^{(k)}, x_i^{(k)})\}_{i=1}^{N_k}$ from environments $k = 1, \dots, K$; significance level α ; minimum number of environments required for hypothesis test K_{\min}

```

 $L_{\max} \leftarrow \text{ceiling}(\max_k N_k / 2)$           /* The maximum number of possible hypothesis tests */
for  $i = 1, \dots, L_{\max}$  do
     $\pi_{2i} \leftarrow \{k \in [K] : N_k \leq 2i\}$     /* Retrieve all environments with at least  $2i$  samples */
    if  $\text{size}(\pi_{2i}) < K_{\min}$  then
        break /* Stop while-loop if we run out of a sufficient number of environments */
     $p_i \leftarrow \text{cond\_indep\_test}(t_{2i-1}^{\pi_{2i}} \perp\!\!\!\perp y_{2i}^{\pi_{2i}} \mid t_{2i}^{\pi_{2i}}, x_{2i-1}^{\pi_{2i}}, x_{2i}^{\pi_{2i}})$  /* Perform independence test */
 $z \leftarrow -2 \sum_{i=1}^{L_{\max}} \log(p_i)$           /* Aggregate p-values */
 $p \leftarrow 1 - \text{cdf}_{\chi^2_{2L}}(z)$           /* Compute global p-value */
return  $p \leq \alpha$ 
    
```

E Further Analysis on the Influence of the Assumptions

In this section, we present more elaboration on the examples of violating the assumptions behind our theory, as discussed in Section 4.1. First, we provide a counter-example that shows how Theorem 1 fails when we have dependent causal mechanisms. Secondly, we demonstrate how we got to our conclusions on having degenerate mechanisms. Finally, we provide insights of when faithfulness violations could occur in an example with a linear-Gaussian structural causal model.

E.1 Dependent Mechanisms

We wish to demonstrate examples of DAGs where the main condition

$$T_j^{(k)} \perp\!\!\!\perp_P Y_i^{(k)} \mid T_i^{(k)}, X_i^{(k)}, X_j^{(k)}$$

in Theorem 1 is violated despite that there is no confounding when some of the causal mechanisms are pairwise dependent. We are able to find examples of violations with all pairwise dependencies, except for $\Theta_X \not\perp\!\!\!\perp_P \Theta_U$. Hence, we conjecture that a dependency between the mechanism of the observed and unobserved confounder does not influence the test proposed by our theory. Figures 7a, 7b, 7c, 8a and 8b show found examples where violations occur between the mechanisms.

E.2 Degenerate Mechanisms

What happens if one or more of the distributions $P(\Theta_T)$, $P(\Theta_Y)$, $P(\Theta_X)$, and $P(\Theta_U)$ are constant across all environments? We investigate these scenarios by first adding Θ_T , Θ_Y , Θ_X and/or Θ_U to the conditioning set in $T_j^{(k)} \perp\!\!\!\perp_P Y_i^{(k)} \mid T_i^{(k)}, X_i^{(k)}, X_j^{(k)}$ - the testable implication for confounding. We then follow the same procedure as for proving Theorem 1 and noting whether this conditional independence still discriminates between cases when U is and is not a confounder. Out of 15 possible cases with degenerate mechanisms, we identify that the theorem fails every time we condition on both Θ_T and Θ_U , as demonstrated in Table 3.

E.3 Faithfulness Violation

What happens if the conditional independencies we test do not correspond to the dependencies in the underlying causal graph? If that is the case, we would fail to detect dependencies implying the presence of confounders. Knowing when a faithfulness violation occurs is not possible, we can only reason about its plausibility. In this section, we first showcase an example where a faithfulness violation occurs in linear-Gaussian structural causal models for particular configurations as well as when the confounder effect sizes – that is γ and λ in (7) – become very large.

It was proved by Meek (1995) that all graphs with discrete and linear-Gaussian data distributions fulfill faithfulness in a measure-theoretic sense; distributions that violate faithfulness have measure zero.

However, even if we restrict T and Y to be categorical we might not want to assume that U or the causal mechanisms follow a discrete distribution. The following example also demonstrates the practical issues stemming from faithfulness violations even when the data is jointly Gaussian.

Example 1. Let $k = 1, \dots, K$ and $i = 1, \dots, N_k$. Consider the structural causal model

$$\begin{aligned} U_i^{(k)} &= \Theta_U^{(k)} + \varepsilon_{U,i}, & \varepsilon_{U,i} &\sim \text{Normal}(0, \sigma_U^2), \\ T_i^{(k)} &= \gamma U_i^{(k)} + \Theta_T^{(k)} + \varepsilon_{T,i}, & \varepsilon_{T,i} &\sim \text{Normal}(0, \sigma_T^2), \\ Y_i^{(k)} &= \lambda U_i^{(k)} + \beta T_i^{(k)} + \Theta_Y^{(k)} + \varepsilon_{Y,i}, & \varepsilon_{Y,i} &\sim \text{Normal}(0, \sigma_Y^2), \end{aligned} \quad (7)$$

where $\Theta_V^{(k)} \sim \text{Normal}(0, \sigma_{\Theta_V}^2)$ and $\varepsilon_V \perp_P \Theta_V^{(k)}$ for $V \in \{T, Y, U\}$. Further, subscript i for the noise variables indicates that they are sampled independently for each observation i . Then, despite the presence of confounding, $T_j^{(k)} \perp_P Y_i^{(k)} \mid T_i^{(k)}$ for any $i \neq j$ when $\sigma_{\Theta_U} = \frac{\sigma_U}{\sigma_T} \sigma_{\Theta_T}$. In the finite-sample setting, it noticeably influences our ability to detect confounding when the distribution parameters come close to this equality, as illustrated in Figure 9.

To create Figure 9, we generate data according to (7) with the following parameters fixed: $\beta = \gamma = \lambda = 1$, $\sigma_{\Theta_Y} = 1$, $\sigma_Y = \sigma_U = 1$ and $\sigma_T = \frac{2}{3}$. Meanwhile, we vary σ_{Θ_T} and σ_{Θ_U} between 0 and 5. We test $T_j^{(k)} \perp_P Y_i^{(k)} \mid T_i^{(k)}$ using the partial correlation (Baba et al., 2004). The experiment is repeated 1000 times with 1000 environments and a significance level $\alpha = 0.05$.

E.4 Derivation of Example 1

We consider the structural causal model in (7). Now, we want to prove that $T_j^{(k)} \perp_P Y_i^{(k)} \mid T_i^{(k)}$ for any $i \neq j$ when $\sigma_{\Theta_U} = \frac{\sigma_U}{\sigma_T} \sigma_{\Theta_T}$. For ease of notation, we will drop the superscript (k) , as the results hold for any k .

Crucially, we note that the partial correlation

$$\rho_{T_j, Y_i \cdot T_i} = \frac{\rho_{T_j, Y_i} - \rho_{T_j, T_i} \rho_{T_i, Y_i}}{\sqrt{1 - \rho_{T_j, T_i}^2} \sqrt{1 - \rho_{T_i, Y_i}^2}}, \quad (8)$$

is zero if and only if $T_j \perp_P Y_i \mid T_i$ when the data is jointly Gaussian (Baba et al., 2004), which is the case for (7) because $p(T_i, Y_i, U_i) = P(Y_i \mid T_i, U_i)P(T_i \mid U_i)P(U_i)$ where each factor is a Gaussian density.

To check when the partial correlation is zero, we need to find out when

$$\rho_{T_j, Y_i} - \rho_{T_j, T_i} \rho_{T_i, Y_i} = 0.$$

Since $\rho_{X,Y} = \frac{\text{Cov}(X,Y)}{\sqrt{\text{Var}(X)\text{Var}(Y)}}$ for some random variables X and Y , we can write this as

$$\rho_{T_j, Y_i} - \rho_{T_j, T_i} \rho_{T_i, Y_i} = \frac{\text{Cov}(T_j, Y_i)}{\sqrt{\text{Var}(T_j)\text{Var}(Y_i)}} - \frac{\text{Cov}(T_j, T_i)}{\sqrt{\text{Var}(T_j)\text{Var}(T_i)}} \frac{\text{Cov}(T_i, Y_i)}{\sqrt{\text{Var}(T_i)\text{Var}(Y_i)}} \quad (9)$$

$$= \frac{\text{Var}(T_i)\text{Cov}(T_j, Y_i) - \text{Cov}(T_j, T_i)\text{Cov}(T_i, Y_i)}{\sqrt{\text{Var}(T_i)^3\text{Var}(Y_i)}}, \quad (10)$$

where we used the fact that $\text{Var}(T_i) = \text{Var}(T_j)$ for any samples i and j .

First, we need to determine all the (co)variances, for which we need to know

$$\begin{aligned} T_i &= \gamma\Theta_U + \gamma\varepsilon_{U,i} + \Theta_T + \varepsilon_{T,i} \\ Y_i &= \lambda\Theta_U + \lambda\varepsilon_{U,i} + \beta\gamma\Theta_U + \beta\gamma\varepsilon_{U,i} + \beta\Theta_T + \beta\varepsilon_{T,i} + \Theta_Y + \varepsilon_{Y,i} \end{aligned}$$

Note that $\mathbb{E}[T_i] = \mathbb{E}[Y_i] = 0$. Consequently, we can write out the covariances, for any i, j , as follows:

$$\begin{aligned} \text{Cov}(T_j, Y_i) &= \mathbb{E}[T_j Y_i] = (\gamma\lambda + \beta\gamma^2)\mathbb{E}[\Theta_U^2] + \beta\mathbb{E}[\Theta_T^2] \\ \text{Cov}(T_j, T_i) &= \mathbb{E}[T_j T_i] = \gamma^2\mathbb{E}[\Theta_U^2] + \mathbb{E}[\Theta_T^2] \\ \text{Cov}(T_i, Y_i) &= \mathbb{E}[T_i Y_i] = (\gamma\lambda + \beta\gamma^2)\mathbb{E}[\Theta_U^2] + (\gamma\lambda + \beta\gamma^2)\mathbb{E}[\varepsilon_U^2] + \beta\mathbb{E}[\Theta_T^2] + \beta\mathbb{E}[\varepsilon_T^2] \\ \text{Var}(T_i) &= \mathbb{E}[T_i T_i] = \gamma^2\mathbb{E}[\Theta_U^2] + \gamma^2\mathbb{E}[\varepsilon_U^2] + \mathbb{E}[\Theta_T^2] + \mathbb{E}[\varepsilon_T^2] \\ \text{Var}(Y_i) &= \mathbb{E}[Y_i Y_i] = 2(\lambda^2 + \beta^2\gamma^2)\mathbb{E}[\Theta_U^2] + 2(\lambda^2 + \beta^2\gamma^2)\mathbb{E}[\varepsilon_U^2] + \beta^2\mathbb{E}[\Theta_T^2] + \beta^2\mathbb{E}[\varepsilon_T^2] + \mathbb{E}[\Theta_Y^2] + \mathbb{E}[\varepsilon_Y^2] \end{aligned}$$

Now, we look at the numerator in (10) and we want to know when it could be zero since that makes the partial correlation zero:

$$\begin{aligned} 0 &= \text{Var}(T_i)\text{Cov}(T_j, Y_i) - \text{Cov}(T_j, T_i)\text{Cov}(T_i, Y_i) \\ &= \gamma\lambda(\mathbb{E}[\Theta_U^2]\mathbb{E}[\varepsilon_T^2] - \mathbb{E}[\varepsilon_U^2]\mathbb{E}[\Theta_T^2]) \end{aligned}$$

The solution is given by

$$\sigma_{\Theta_U} = \frac{\sigma_U}{\sigma_T} \sigma_{\Theta_T}, \quad (11)$$

where the square root of the second moments are equal to the standard deviations. This is the same equality as demonstrated in the example.

E.5 Asymptotic Behavior of Partial Correlation

We also look at the partial correlation and ask what happens when the confounder effect sizes γ or λ become very large. The numerator in (10) grows linearly with respect to both γ and λ , and the other variances can be rewritten as

$$\begin{aligned} \text{Cov}(T_j, T_i) &= \gamma^2\mathbb{E}[\Theta_U^2] + O(1) \\ \text{Cov}(T_i, Y_i) &= (\gamma\lambda + \beta\gamma^2)(\mathbb{E}[\Theta_U^2] + \mathbb{E}[\varepsilon_U^2]) + O(1) \\ \text{Var}(T_i) &= \gamma^2(\mathbb{E}[\Theta_U^2] + \mathbb{E}[\varepsilon_U^2]) + O(1) \\ \text{Var}(Y_i) &= 2(\lambda^2 + \beta^2\gamma^2)(\mathbb{E}[\Theta_U^2] + \mathbb{E}[\varepsilon_U^2]) + O(1) \end{aligned}$$

where $O(1)$ is a constant with respect to γ and λ .

We rewrite the partial correlation (8) as

$$\rho_{T_j, Y_i, T_i} = \frac{(\text{Var}(T_i)\text{Cov}(T_j, Y_i) - \text{Cov}(T_j, T_i)\text{Cov}(T_i, Y_i)) / \sqrt{\text{Var}(T_i)^3 \text{Var}(Y_i)}}{\sqrt{1 - \frac{\text{Cov}(T_j, T_i)^2}{\text{Var}(T_i)^2}} \sqrt{1 - \frac{\text{Cov}(T_i, Y_i)^2}{\text{Var}(T_i)\text{Var}(Y_i)}}}.$$

Assuming that all second moments are non-zero and finite, it is possible to show that

$$\rho_{T_j, Y_i, T_i} \propto \begin{cases} \gamma^{-3} & \text{for } |\gamma| \gg 1, \\ 1 & \text{for } |\lambda| \gg 1 \end{cases}.$$

Hence, when either $|\gamma|$ or $|\lambda|$ goes to infinity we have

$$\begin{aligned} \rho_{T_j, Y_i, T_i} &\xrightarrow{|\gamma| \rightarrow \infty} 0 \\ \rho_{T_j, Y_i, T_i} &\xrightarrow{|\lambda| \rightarrow \infty} C \text{ for some } C \in [-1, 1] \end{aligned}$$

Note that C could be zero, for instance when $\sigma_{\Theta_U} = \frac{\sigma_U}{\sigma_T} \sigma_{\Theta_T}$, although we demonstrate with simulation studies in Appendix G a case where C is non-zero as well.

Interestingly, in this case, the bias from estimating the causal effect without adjusting for the confounder U is

$$\mathbb{E}[Y \mid do(T)] - \mathbb{E}[Y \mid T] = \beta T - (\beta T + \frac{\lambda}{\gamma} T) = -\frac{\lambda}{\gamma} T. \quad (12)$$

We note that when $\gamma \rightarrow \infty$ the bias goes to zero, similar to the partial correlation. Meanwhile, the bias increases with λ which also is consistent with the asymptotic behavior of the partial correlation as $\lambda \rightarrow \infty$.

F Generation of Twins Semi-synthetic Dataset

We use data from twin births in the USA between 1989-1991 (Almond et al., 2005; Louizos et al., 2017) to construct an observational dataset with a known causal structure. The dataset contains 46 covariates related to pregnancy, birth, and parents, out of which we select ten as potential confounders in our experiments. Many covariates are highly imbalanced and have low variance, some even on the border of being constant. Due to this, we wish to exclude those in data generation. The selection is performed by first excluding any binary variables from the list of covariates, and then further removing the remaining ones that have an empirical variance smaller than one.

In the end, the following covariates are used from the Twins dataset for our data generation: birth month, father’s age, mom’s age, mom’s education, mom’s place of birth, number of prenatal visits, number of live births before twins, the total number of births before twins, period of gestation, state of birth occurrence, and state of registered residence. Note that all of these are reported as categorical/discrete variables in the dataset.

Among the covariates, we use the state in which the birth took place as environment label, hence obtaining 51 different environments. We simulate a continuous treatment and outcome by randomly selecting $p \in [1, \dots, 10]$ features (X_1, X_2, \dots, X_p) and a set of functions to generate the data as follows:

$$T = \sum_{d=1}^p \alpha_d f_d(X_{d,\text{scaled}}) + \varepsilon_T \quad \text{and} \quad Y = \sum_{d=1}^p \beta_d g_d(X_{d,\text{scaled}}) + \delta T + \varepsilon_Y \quad (13)$$

For each d , α_d is sampled from a uniform distribution $\text{Unif}(1, 5)$, β_d is sampled from a uniform distribution $\text{Unif}(1, 5)$, and f_d and g_d are sampled from the set of functions $\{\tanh(x), x, x^2\}$ with equal probability. The treatment effect, δ , is also randomly sampled from a uniform distribution $\text{Unif}(1, 2)$, and we have noise variables $\varepsilon_T \sim \text{Normal}(0, 1/4)$ and $\varepsilon_Y \sim \text{Normal}(0, 1/4)$. The features from the Twins dataset are also scaled as

$$X_{d,\text{scaled}} = 5 * (X_d - \text{mean}(X_d)) / (\max(X_d) - \min(X_d)), \quad (14)$$

where mean/max/min are taken over all observed values of the covariate X_d . Note that the functions are fixed across all environments in this setup, and variations between environments only stem from the real-world distribution shifts of the covariates between birth states.

G Additional Experiments

We present additional simulation studies, mainly replicating the experiments on synthetic data from Section 5.1 with continuous data. In addition, we further investigate the asymptotic behavior of the partial correlation from Appendix E.3 with both the binary and continuous data.

The continuous data is generated from a linear-Gaussian DAG as described in (7). Unless otherwise stated, we use $\beta = 1$, $\sigma_T = \sigma_U = \sigma_Y = 1$, $\sigma_{\Theta_T} = \sigma_{\Theta_Y} = 1$ and $\sigma_{\Theta_U} = 5$. To vary the influence of the hidden confounder, we can adjust either γ or λ . We test $T_j^{(k)} \perp\!\!\!\perp_P Y_i^{(k)} \mid T_i^{(k)}$ using the partial correlation (Baba et al., 2004) with $N_k = 2$ samples per environment.

For the first experiment, we vary the number of environments and the confounder influence by setting $\gamma = \lambda$. In the main part of the paper, we only considered what happens when varying λ with $\gamma = 1$. Similarly, we do the same experiment with the binary data for comparison. The results are seen in Figure 10. Notably, the probability of detecting

hidden confounding starts decreasing when $\gamma = \lambda$ goes above a certain threshold. This is consistent with our previous conclusions from Appendix E.3, where we noted that partial correlation is proportional to γ^{-3} for $\gamma \gg 1$ while remaining constant for $\lambda \gg 1$. Hence, we would expect the partial correlation to shrink as both γ and λ grow. Notably, the effect is more pronounced with the continuous data although it can also be seen with the binary data.

Secondly, we perform the experiment with continuous data where we only vary λ while fixing $\gamma = 1$. The results are shown in Figure 11, we note that the probability of detection no longer decreases as the confounder effect size increases. The results with binary data are also shown again for comparison. Once again, this is predicted by the asymptotic behavior of the partial correlation.

Finally, we compare our statistical testing procedure to testing $Y \perp_P E \mid T$ with continuous data in Figure 13. We run the experiment with 10000 environments, 100 samples per environment, and $\sigma_{\Theta_U} = 10$ to avoid the issues of faithfulness violations which we have discussed before. Similar to the case with binary data, in Figure 12b, we see that the probability of false detection when testing $Y \perp_P E \mid T$ grows as the standard deviation of Θ_Y increases. Meanwhile, we do not observe this problem in our testing procedure. The case when confounding is present is shown in Figure 12a to confirm that our method is able to detect confounding. For completion, we also include a case where $\lambda = 10$ (confounding is present) for the binary data experiment presented in the main part of the paper, this is shown in Figure 13a.

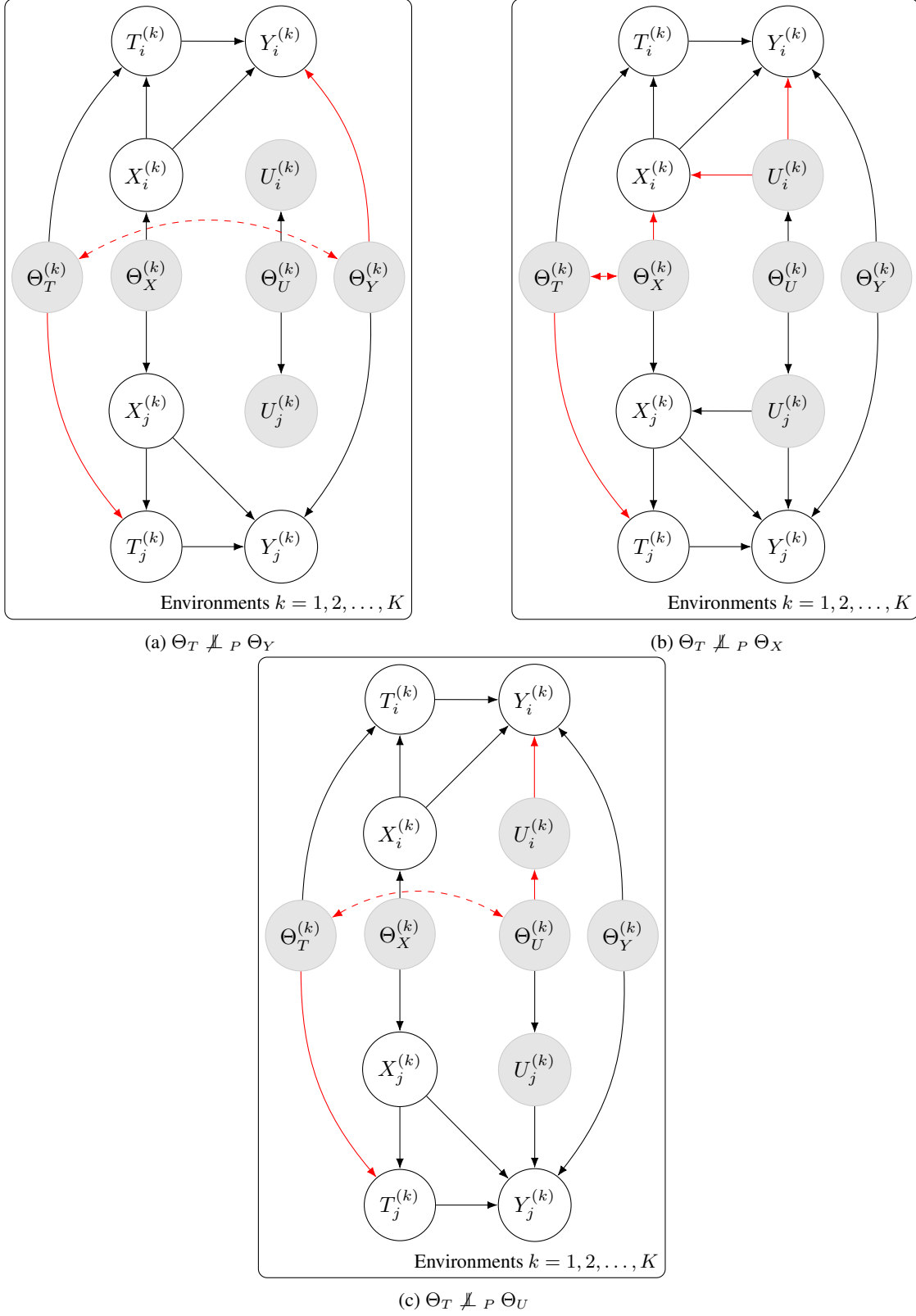


Figure 7: Violations of $T_j^{(k)} \perp_P Y_i^{(k)} \mid T_i^{(k)}, X_i^{(k)}, X_j^{(k)}$ with dependent mechanisms despite that X is a valid adjustment set for estimating $P(Y \mid do(T))$. Open paths between $T_j^{(k)}$ and $Y_i^{(k)}$ after conditioning on T_i, X_i and X_j are marked in red.

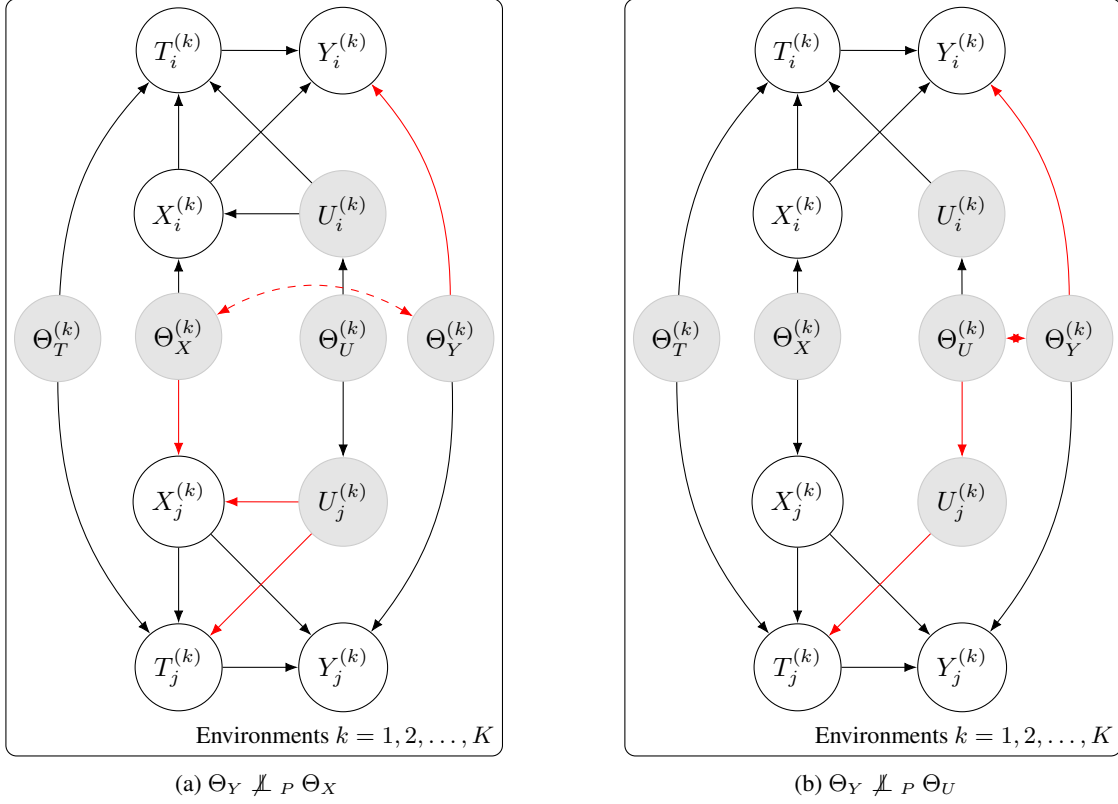


Figure 8: Violations of $T_j^{(k)} \perp_P Y_i^{(k)} \mid T_i^{(k)}, X_i^{(k)}, X_j^{(k)}$ with dependent mechanisms despite that X is a valid adjustment set for estimating $P(Y \mid do(T))$. Open paths between $T_j^{(k)}$ and $Y_i^{(k)}$ after conditioning on T_i, X_i and X_j are marked in red.

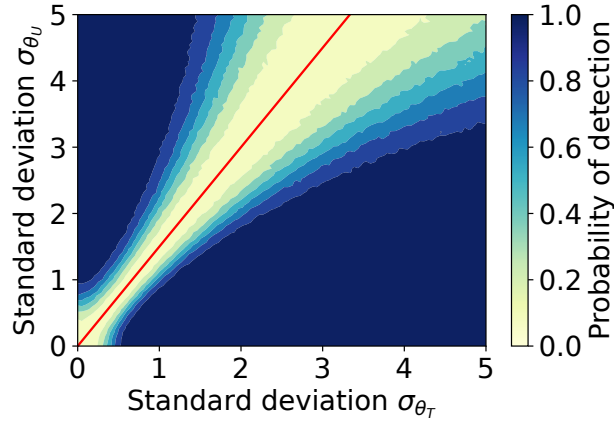


Figure 9: Faithfulness violation from Example 1. Varying σ_{Θ_T} and σ_{Θ_U} with $\sigma_T = \frac{2}{3}$ and $\sigma_U = 1$, the probability for detecting confounding goes to zero as we get closer to $\sigma_{\Theta_U} = \frac{\sigma_U}{\sigma_T} \sigma_{\Theta_T}$ (red line).

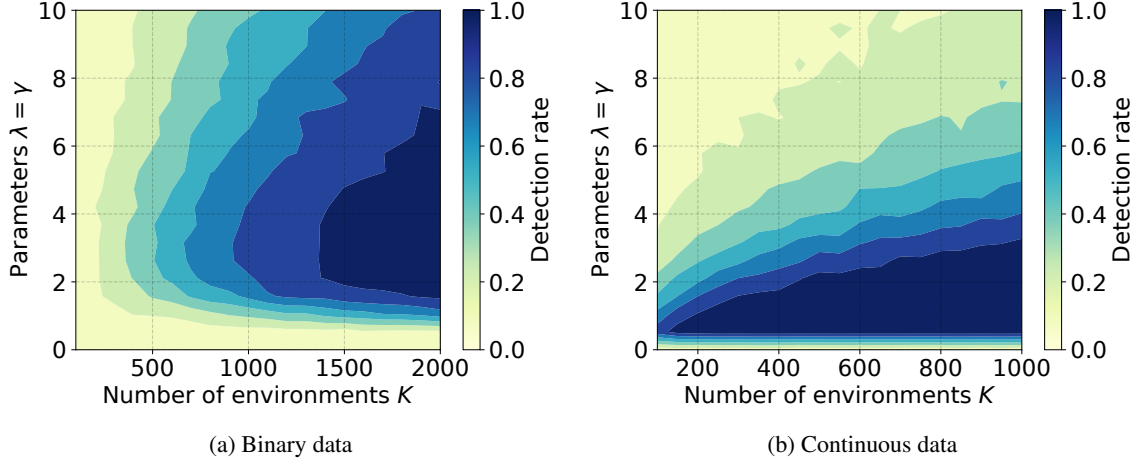


Figure 10: Probability of detecting hidden confounding for varying the number of environments K and confounder effect sizes where $\lambda = \gamma$ are varied jointly. 500 repetitions.

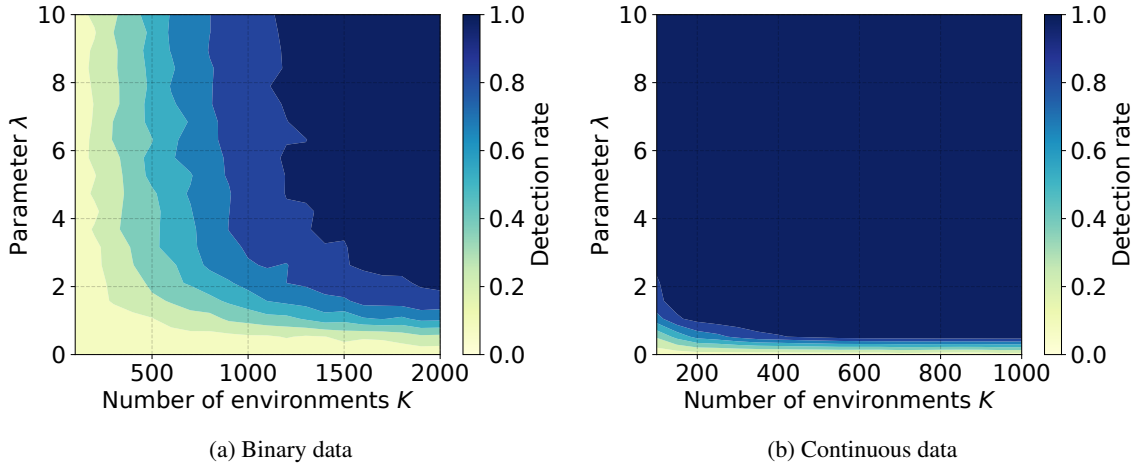


Figure 11: Probability of detecting hidden confounding for varying the number of environments K and confounder effect sizes where λ is varied while $\gamma = 1$ is fixed. 500 repetitions

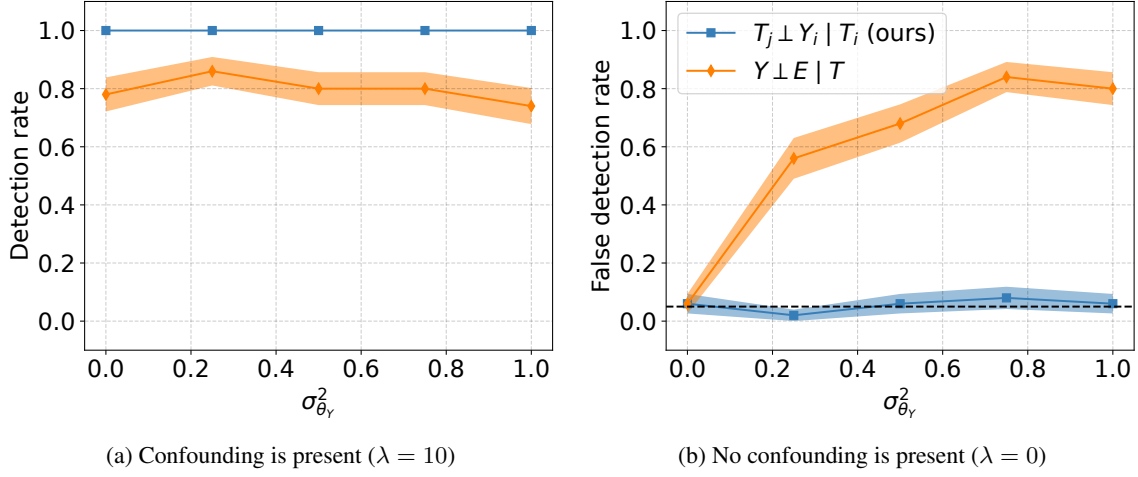


Figure 12: Comparison on continuous linear-Gaussian data between the proposed procedure and an alternative testing procedure by varying the standard deviation of Θ_Y in both the presence and absence of confounding. The black dashed line corresponds to the desired type 1 error control $\alpha = 0.05$. The shaded area shows the standard error from 50 repetitions.

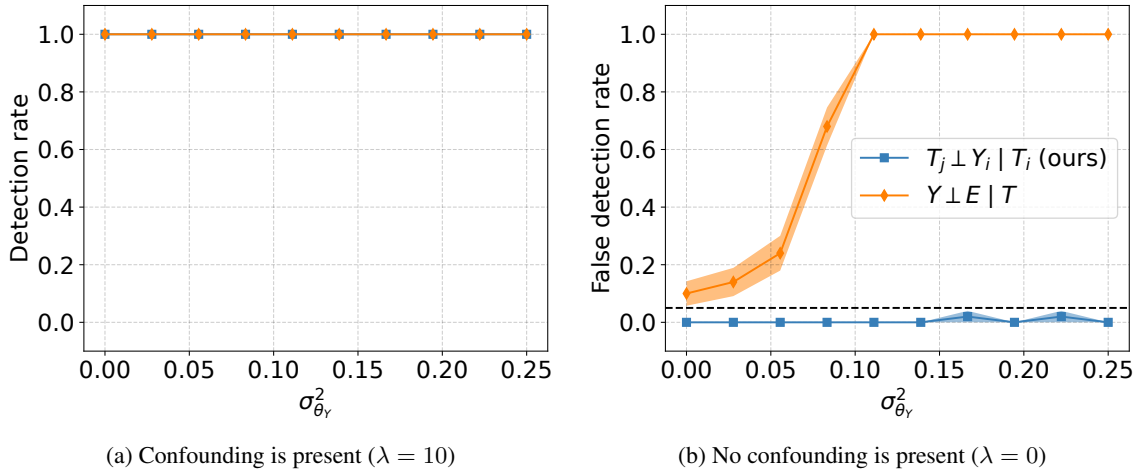


Figure 13: Comparison on binary data between the proposed procedure and an alternative testing procedure by varying the standard deviation of Θ_Y in both the presence and absence of confounding. The black dashed line corresponds to the desired type 1 error control $\alpha = 0.05$. The shaded area shows the standard error from 50 repetitions.

Table 1: Conditional d-separations in combinations of DAGs with variables (T, Y, X, U) . For the d-separation, (\checkmark) indicates that it holds and (\times) otherwise. The shaded rows are the cases where U is a confounder to T and Y in \mathcal{G} .

id	$X \perp\!\!\!\perp T$	$X \perp\!\!\!\perp Y$	$T \perp\!\!\!\perp Y$	$U \perp\!\!\!\perp T$	$U \perp\!\!\!\perp Y$	$U \perp\!\!\!\perp X$	$T_j^{(k)} \perp_d Y_i^{(k)} \mid T_i^{(k)}, X_i^{(k)}, X_j^{(k)}$	U is confounder
1	\rightarrow	\rightarrow	\rightarrow	\rightarrow	\rightarrow	\rightarrow	\times	\checkmark
2	\rightarrow	\rightarrow	\rightarrow	\rightarrow	\rightarrow	\rightarrow	\times	\checkmark
3	\rightarrow	\rightarrow	\rightarrow	\rightarrow	\rightarrow	\rightarrow	\times	\checkmark
4	\rightarrow	\rightarrow	\rightarrow	\rightarrow		\rightarrow	\checkmark	\times
5	\rightarrow	\rightarrow	\rightarrow	\rightarrow		\rightarrow	\checkmark	\times
6	\rightarrow	\rightarrow	\rightarrow	\rightarrow			\checkmark	\times
7	\rightarrow	\rightarrow	\rightarrow	\leftarrow	\rightarrow	\leftarrow	\checkmark	\times
8	\rightarrow	\rightarrow	\rightarrow	\leftarrow	\rightarrow		\checkmark	\times
9	\rightarrow	\rightarrow	\rightarrow	\leftarrow	\leftarrow	\leftarrow	\checkmark	\times
10	\rightarrow	\rightarrow	\rightarrow	\leftarrow	\leftarrow		\checkmark	\times
11	\rightarrow	\rightarrow	\rightarrow	\leftarrow		\leftarrow	\checkmark	\times
12	\rightarrow	\rightarrow	\rightarrow	\leftarrow			\checkmark	\times
13	\rightarrow	\rightarrow	\rightarrow		\rightarrow	\rightarrow	\checkmark	\times
14	\rightarrow	\rightarrow	\rightarrow		\rightarrow	\leftarrow	\checkmark	\times
15	\rightarrow	\rightarrow	\rightarrow		\rightarrow		\checkmark	\times
16	\rightarrow	\rightarrow	\rightarrow		\leftarrow	\leftarrow	\checkmark	\times
17	\rightarrow	\rightarrow	\rightarrow		\leftarrow		\checkmark	\times
18	\rightarrow	\rightarrow	\rightarrow			\rightarrow	\checkmark	\times
19	\rightarrow	\rightarrow	\rightarrow			\leftarrow	\checkmark	\times
20	\rightarrow	\rightarrow	\rightarrow				\checkmark	\times
21	\rightarrow	\rightarrow		\rightarrow	\rightarrow	\rightarrow	\times	\checkmark
22	\rightarrow	\rightarrow		\rightarrow	\rightarrow	\leftarrow	\times	\checkmark
23	\rightarrow	\rightarrow		\rightarrow	\rightarrow		\times	\checkmark
24	\rightarrow	\rightarrow		\rightarrow		\rightarrow	\checkmark	\times
25	\rightarrow	\rightarrow		\rightarrow		\leftarrow	\checkmark	\times
26	\rightarrow	\rightarrow		\rightarrow			\checkmark	\times
27	\rightarrow	\rightarrow		\leftarrow	\rightarrow	\leftarrow	\checkmark	\times
28	\rightarrow	\rightarrow		\leftarrow	\rightarrow		\checkmark	\times
29	\rightarrow	\rightarrow		\leftarrow	\leftarrow	\leftarrow	\checkmark	\times
30	\rightarrow	\rightarrow		\leftarrow	\leftarrow		\checkmark	\times
31	\rightarrow	\rightarrow		\leftarrow		\leftarrow	\checkmark	\times
32	\rightarrow	\rightarrow		\leftarrow			\checkmark	\times
33	\rightarrow	\rightarrow			\rightarrow	\rightarrow	\checkmark	\times
34	\rightarrow	\rightarrow			\rightarrow	\leftarrow	\checkmark	\times
35	\rightarrow	\rightarrow			\rightarrow		\checkmark	\times
36	\rightarrow	\rightarrow			\leftarrow	\leftarrow	\checkmark	\times
37	\rightarrow	\rightarrow			\leftarrow		\checkmark	\times
38	\rightarrow	\rightarrow				\rightarrow	\checkmark	\times
39	\rightarrow	\rightarrow				\leftarrow	\checkmark	\times
40	\rightarrow	\rightarrow					\checkmark	\times

Table 2: Conditional d-separations in combinations of DAGs with variables (T, Y, U) (this excludes any observed confounder X). For the d-separation, (\checkmark) indicates that it holds and (\times) otherwise. The shaded rows are the cases where U is a confounder to T and Y in \mathcal{G} .

id	$T \rightarrow Y$	$U \rightarrow T$	$U \rightarrow Y$	$T_j^{(k)} \perp_d Y_i^{(k)} \mid T_i^{(k)}$	$T_j^{(k)} \perp_d Y_i^{(k)} \mid Y_j^{(k)}$	U is confounder	Y ancestor of T
1	\rightarrow	\rightarrow	\rightarrow	\times	\times	\checkmark	\times
2	\rightarrow	\rightarrow		\checkmark	\times	\times	\times
3	\rightarrow	\leftarrow	\rightarrow	\checkmark	\times	\times	\times
4	\rightarrow	\leftarrow	\leftarrow	\checkmark	\times	\times	\times
5	\rightarrow	\leftarrow		\checkmark	\times	\times	\times
6	\rightarrow		\rightarrow	\checkmark	\times	\times	\times
7	\rightarrow		\leftarrow	\checkmark	\times	\times	\times
8	\rightarrow			\checkmark	\times	\times	\times
9	\leftarrow	\rightarrow	\rightarrow	\times	\times	\checkmark	\checkmark
10	\leftarrow	\rightarrow	\leftarrow	\times	\checkmark	\times	\checkmark
11	\leftarrow	\rightarrow		\times	\checkmark	\times	\checkmark
12	\leftarrow	\leftarrow	\leftarrow	\times	\checkmark	\times	\checkmark
13	\leftarrow	\leftarrow		\times	\checkmark	\times	\checkmark
14	\leftarrow		\rightarrow	\times	\checkmark	\times	\checkmark
15	\leftarrow		\leftarrow	\times	\checkmark	\times	\checkmark
16	\leftarrow			\times	\checkmark	\times	\checkmark
17		\rightarrow	\rightarrow	\times	\times	\checkmark	\times
18		\rightarrow	\leftarrow	\times	\checkmark	\times	\checkmark
19		\rightarrow		\checkmark	\checkmark	\times	\times
20		\leftarrow	\rightarrow	\checkmark	\times	\times	\times
21		\leftarrow	\leftarrow	\checkmark	\checkmark	\times	\times
22		\leftarrow		\checkmark	\checkmark	\times	\times
23			\rightarrow	\checkmark	\checkmark	\times	\times
24			\leftarrow	\checkmark	\checkmark	\times	\times
25				\checkmark	\checkmark	\times	\times

